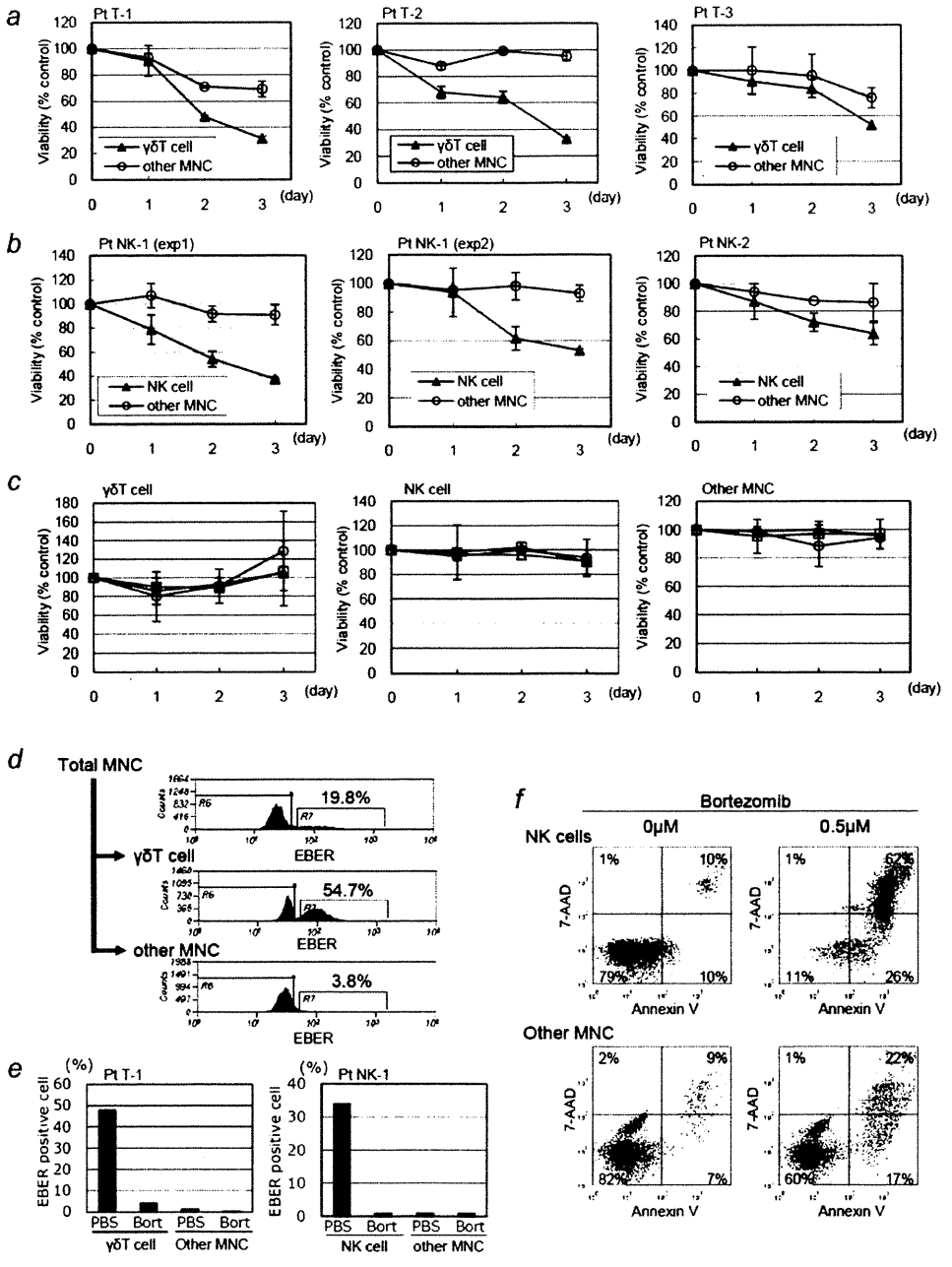

Figure 6. Bortezomib decreases the viability of EBV-infected cells from patients with EBV-associated diseases. (*a, b, c*) Bortezomib (0.5 μM) was administered to each sample of cells, and the viable cells were counted for 3 days. (*a*) γδT cells and other MNCs from three patients (Patients T-1, T-2, and T-3) with hydroa vacciniforme-like lymphoma, (*b*) NK cells and other MNCs from two patients (Patients NK-1, and NK-2) with NK cell-type chronic active EBV infection, and (*c*) γδT cell, NK cell, and non-γδT, non-NK cell (other MNC) from three healthy donors were separated by magnetic sorting. For Patient NK-1, experiments were performed twice on different visits (exp.1 and exp.2). Bars indicate standard errors. (*d*) EBER-positive cells of Patient T-1 with hydroa vacciniforme-like lymphoma were quantified using a FISH assay on unsorted MNCs (total MNCs), the γδT cell fraction (γδT cell), and the non-γδT cell fraction (other MNCs). (*e*) The EBER-positive rate of each sorted cells from Patient T-1 (left) and Patient NK-1 (right) were quantified using a FISH assay after 3 days treatment with bortezomib or PBS. (*f*) NK cells and other MNCs of Patient NK-1, with NK cell-type chronic active EBV infection were separated by magnetic sorting. Cells were treated with 0.5 μM bortezomib for 24 hr and analyzed by flow cytometry. Viable cells were defined as those negative for annexin V-PE and 7-AAD staining, and early apoptotic cells were defined as those positive for annexin V-PE and negative for 7-AAD staining.

The existence of EBV may have little effect on cell death induced by bortezomib. In a previous study, the killing effect of bortezomib was not different between EBV-positive and -negative Burkitt lymphoma cell lines,[8,41] although Zou *et al.*[8] reported that bortezomib had a greater effect in B cell lines with latency type III than those with Type I. The effect of bortezomib may be different in cells with different latency types due to distinct patterns of viral gene expression. The existence of EBV may have some effect on bortezomib because LMP1 is known to activate NF-κB.[42] In the study by Zou *et al.*,[8] however, transfection of LMP1 into an EBV-negative B cell line did not change the sensitivity to bortezomib. The EBV-positive T and NK cell lines used in our study are classified as latency type II[25] and express LMP1. Bortezomib seemed to have little impact on LMP1-mediated NF-κB activation because the presence of EBV did not influence its effects in our study. Comparing cell lines that are naturally EBV positive with derivative cell lines that have lost EBV is necessary to prove that EBV does not affect the outcome of bortezomib treatment. However, establishing such EBV-depleted cell lines is very difficult and, to our knowledge, there are no existing EBV-depleted T- or NK-cell lines. Alternatively, we compared EBV-negative cell lines and those that have been infected with EBV *in vitro*. We admit that this is an artificial system that may have limited relevance.

Bortezomib induced lytic infection only in T cell lines. Inhibition of the NF-κB pathway has been shown to induce the EBV lytic cycle.[43] Although the reason for the difference in lytic induction between T and NK cell lines is unclear, T cell lines seem to express lytic infection genes more often than NK cell lines, consistent with our previous report.[25] Histone deacetylase inhibitors, such as butyric acid and valproic acid, and phorbol 12-myristate 13-acetate are reported to induce an EBV lytic cycle in B cell and epithelial cell lines.[5,26] To our knowledge, however, no agent induces a lytic cycle in EBV-positive NK cell lines. We administered valproic acid, a class I histone deacetylase inhibitor, to NK-cell lymphoma cell lines. Lytic induction was not induced in the NK cell lines (data not shown).

Such lytic induction could contribute to the decreased viability of T cell lines. However, this lytic induction is not a major mechanism of bortezomib-induced cell death because no significant difference was observed in its effect between T and NK cell lines, or between EBV-positive and -negative cell lines. In SNT-16 cells, bortezomib induced a marked decrease in viability, and the recovery in viability following administration of a pan-caspase inhibitor was incomplete (Fig. 3*c*). Thus, the induction of lytic infection by bortezomib could play a partial role in this cell line. Additionally, this result suggests the potential utility of bortezomib as a novel strategy against EBV-positive T cell lymphoma. In EBV-infected T cells, a few latent genes with low antigenicity are expressed.[25] Moreover, the increased expression of lytic proteins, which are generally antigenic, can be recognized in virus-specific cytotoxic T lymphocytes, resulting in lysis of EBV-infected T cells.

Bortezomib killed EBV-infected γδT cells of hydroa vacciniforme-like lymphoma and EBV-infected NK cells of chronic active EBV infection. Taken together with the flow cytometry results, bortezomib induced apoptosis in EBV-infected immortalized cells. These results indicate that bortezomib may be an effective therapy against EBV-associated T and NK lymphoma/lymphoproliferative diseases. We administered 0.5 μM bortezomib to peripheral blood cells in an *ex vivo* study. This concentration is approximately equal to the plasma concentration after administering 1.3 mg/m^2 bortezomib in a recent Phase I and II study of multiple myeloma.[44]

Although recent studies have shown that the effect of bortezomib could be enhanced synergistically in combination with a histone deacetylase inhibitor,[45–47] further studies with appropriate *in vivo* models are essential to confirm this possibility. EBV infects only humans and no good animal models exist, although recently, humanized mouse models with reconstituted human lymphocytes and EBV infection have been reported.[48–50] Despite the complexity of this mouse model, it could be useful for evaluating new therapies, including molecular targeted therapy. The *ex vivo* administration model, coupled with magnetic sorting, is a convenient method to evaluate molecular targeted therapy against EBV-associated lymphoma.

In conclusion, bortezomib killed T/NK lymphoma cells by inducing apoptosis. No significant difference in killing was observed between EBV-positive and -negative cell lines, although bortezomib induced lytic infection in EBV-infected T cells. Following *ex vivo* administration, bortezomib had a greater killing effect on EBV-positive cells than other MNCs. These results give rationale for the use of bortezomib on T/NK lymphomas, although existence of EBV may have little effect on cell death induced by bortezomib.

Acknowledgements

We thank Norio Shimizu (Tokyo Medical and Dental University) and Ayako Demachi-Okamura (Aichi Cancer Center) for the SNK-6, SNT-13 and SNT-16 cell lines. KAI3 and KHYG-1 were obtained from the Japanese Collection of Research Bioresources. We also thank Millennium Pharmaceuticals Inc. for providing the bortezomib.

All authors have no conflict.

References

1. Cohen JI. Epstein-Barr virus infection. *N Engl J Med* 2000;343:481–92.
2. Quintanilla-Martinez L, Kumar H, Jaffe ES. EBV$^+$ T-cell lymphoma of childhood. In: Jaffe ES, Harris NL, Stein H, eds. WHO classification of tumours of haematopoietic and lymphoid tissues, 4th edn. Lyon: IARC Press, 2008278–28.
3. Rickinson AB, Kieff E. Epstein-Barr virus. In: Knipe DM, Howley PM, eds. Fields virology, vol. 2. Philadelphia, PA: Lippincott Williams & Wilkins, 20072655–700.
4. Williams H, Crawford DH. Epstein-Barr virus: the impact of scientific advances on clinical practice. *Blood* 2006;107:862–9.

5. Kieff ED, Rickinson AV. Epstein-Barr virus and its replication. In: Knipe DM, Howley PM, eds. Fields virology, vol.2. Philadelphia, PA: Lippincott Williams & Wilkins, 2007.2603–54.
6. Cartron G, Watier H, Golay J, Solal-Celigny P. From the bench to the bedside: ways to improve rituximab efficacy. *Blood* 2004;104:2635–42.
7. Heslop HE. How I treat EBV lymphoproliferation. *Blood* 2009;114: 4002–8.
8. Zou P, Kawada J, Pesnicak L, Cohen JI. Bortezomib induces apoptosis of Epstein-Barr virus (EBV)-transformed B cells and prolongs survival of mice inoculated with EBV-transformed B cells. *J Virol* 2007;81: 10029–36.
9. Adams J. Proteasome inhibition: a novel approach to cancer therapy. *Trends Mol Med* 2002;8:S49–54.
10. Orlowski RZ, Eswara JR, Lafond-Walker A, Grever MR, Orlowski M, Dang CV. Tumor growth inhibition induced in a murine model of human Burkitt's lymphoma by a proteasome inhibitor. *Cancer Res* 1998;58: 4342–8.
11. Zhang XM, Lin H, Chen C, Chen BD. Inhibition of ubiquitin-proteasome pathway activates a caspase-3-like protease and induces Bcl-2 cleavage in human M-07e leukaemic cells. *Biochem J* 1999;340(Pt 1):127–33.
12. Jackson G, Einsele H, Moreau P, Miguel JS. Bortezomib, a novel proteasome inhibitor, in the treatment of hematologic malignancies. *Cancer Treat Rev* 2005;31: 591–602.
13. Richardson PG, Mitsiades C, Hideshima T, Anderson KC. Bortezomib: proteasome inhibition as an effective anticancer therapy. *Annu Rev Med* 2006;57:33–47.
14. Paramore A, Frantz S. Bortezomib. *Nat Rev Drug Discov* 2003;2:611–2.
15. Fu DX, Tanhehco YC, Chen J, Foss CA, Fox JJ, Lemas V, Chong JM, Ambinder RF, Pomper MG. Virus-associated tumor imaging by induction of viral gene expression. *Clin Cancer Res* 2007;13:1453–8.
16. Pulvertaft JV. A study of malignant tumours in Nigeria by short-term tissue culture. *J Clin Pathol* 1965;18:261–73.
17. Zhang Y, Nagata H, Ikeuchi T, Mukai H, Oyoshi MK, Demachi A, Morio T, Wakiguchi H, Kimura N, Shimizu N, Yamamoto K. Common cytological and cytogenetic features of Epstein-Barr virus (EBV)-positive natural killer (NK) cells and cell lines derived from patients with nasal T/NK-cell lymphomas, chronic active EBV infection and hydroa vacciniforme-like eruptions. *Br J Haematol* 2003;121:805–14.
18. Tsuge I, Morishima T, Morita M, Kimura H, Kuzushima K, Matsuoka H. Characterization of Epstein-Barr virus (EBV)-infected natural killer (NK) cell proliferation in patients with severe mosquito allergy; establishment of an IL-2-dependent NK-like cell line. *Clin Exp Immunol* 1999;115:385–92.
19. Kaplan J, Tilton J, Peterson WD, Jr. Identification of T cell lymphoma tumor antigens on human T cell lines. *Am J Hematol* 1976;1:219–23.
20. Yagita M, Huang CL, Umehara H, Matsuo Y, Tabata R, Miyake M, Konaka Y, Takatsuki K. A novel natural killer cell line (KHYG-1) from a patient with aggressive natural killer cell leukemia carrying a p53 point mutation. *Leukemia* 2000;14:922–30.
21. Miyoshi I, Kubonishi I, Yoshimoto S, Akagi T, Ohtsuki Y, Shiraishi Y, Nagata K, Hinuma Y. Type C virus particles in a cord T-cell line derived by co-cultivating normal human cord leukocytes and human leukaemic T cells. *Nature* 1981;294:770–1.
22. Fujiwara S, Ono Y. Isolation of Epstein-Barr virus-infected clones of the human T-cell line MT-2: use of recombinant viruses with a positive selection marker. *J Virol* 1995;69:3900–3.
23. Robertson MJ, Cochran KJ, Cameron C, Le JM, Tantravahi R, Ritz J. Characterization of a cell line, NKL, derived from an aggressive human natural killer cell leukemia. *Exp Hematol* 1996;24:406–15.
24. Isobe Y, Sugimoto K, Matsuura I, Takada K, Oshimi K. Epstein-Barr virus renders the infected natural killer cell line, NKL resistant to doxorubicin-induced apoptosis. *Br J Cancer* 2008;99:1816–22.
25. Iwata S, Wada K, Tobita S, Gotoh K, Ito Y, Demachi-Okamura A, Shimizu N, Nishiyama Y, Kimura H. Quantitative analysis of Epstein-Barr virus (EBV)-related gene expression in patients with chronic active EBV infection. *J Gen Virol* 2010;91:42–50.
26. Kubota N, Wada K, Ito Y, Shimoyama Y, Nakamura S, Nishiyama Y, Kimura H. One-step multiplex real-time PCR assay to analyse the latency patterns of Epstein-Barr virus infection. *J Virol Methods* 2008;147: 26–36.
27. Patel K, Whelan PJ, Prescott S, Brownhill SC, Johnston CF, Selby PJ, Burchill SA. The use of real-time reverse transcription-PCR for prostate-specific antigen mRNA to discriminate between blood samples from healthy volunteers and from patients with metastatic prostate cancer. *Clin Cancer Res* 2004;10:7511–9.
28. Kimura H, Miyake K, Yamauchi Y, Nishiyama K, Iwata S, Iwatsuki K, Gotoh K, Kojima S, Ito Y, Nishiyama Y. Identification of Epstein-Barr virus (EBV)-infected lymphocyte subtypes by flow cytometric in situ hybridization in EBV-associated lymphoproliferative diseases. *J Infect Dis* 2009;200:1078–87.
29. Kimura H, Hoshino Y, Hara S, Sugaya N, Kawada J, Shibata Y, Kojima S, Nagasaka T, Kuzushima K, Morishima T. Differences between T cell-type and natural killer cell-type chronic active Epstein-Barr virus infection. *J Infect Dis* 2005;191:531–9.
30. Kimura H, Hoshino Y, Kanegane H, Tsuge I, Okamura T, Kawa K, Morishima T. Clinical and virologic characteristics of chronic active Epstein-Barr virus infection. *Blood* 2001;98:280–6.
31. Kimura H, Morishima T, Kanegane H, Ohga S, Hoshino Y, Maeda A, Imai S, Okano M, Morio T, Yokota S, Tsuchiya S, Yachie A, et al. Prognostic factors for chronic active Epstein-Barr virus infection. *J Infect Dis* 2003;187:527–33.
32. Shen L, Au WY, Guo T, Wong KY, Wong ML, Tsuchiyama J, Yuen PW, Kwong YL, Liang RH, Srivastava G. Proteasome inhibitor bortezomib-induced apoptosis in natural killer (NK)-cell leukemia and lymphoma: an in vitro and in vivo preclinical evaluation. *Blood* 2007;110: 469–70.
33. Shen L, Au WY, Wong KY, Shimizu N, Tsuchiyama J, Kwong YL, Liang RH, Srivastava G. Cell death by bortezomib-induced mitotic catastrophe in natural killer lymphoma cells. *Mol Cancer Ther* 2008;7:3807–15.
34. Lee J, Suh C, Kang HJ, Ryoo BY, Huh J, Ko YH, Eom HS, Kim K, Park K, Kim WS. Phase I study of proteasome inhibitor bortezomib plus CHOP in patients with advanced, aggressive T-cell or NK/T-cell lymphoma. *Ann Oncol* 2008;19:2079–83.
35. Zinzani PL, Musuraca G, Tani M, Stefoni V, Marchi E, Fina M, Pellegrini C, Alinari L, Derenzini E, de Vivo A, Sabattini E, Pileri S, et al. Phase II trial of proteasome inhibitor bortezomib in patients with relapsed or refractory cutaneous T-cell lymphoma. *J Clin Oncol* 2007;25:4293–7.
36. Hideshima T, Richardson P, Chauhan D, Palombella VJ, Elliott PJ, Adams J, Anderson KC. The proteasome inhibitor PS-341 inhibits growth, induces apoptosis, and overcomes drug resistance in human multiple myeloma cells. *Cancer Res* 2001; 61:3071–6.
37. Kim K, Ryu K, Ko Y, Park C. Effects of nuclear factor-kappaB inhibitors and its implication on natural killer T-cell lymphoma cells. *Br J Haematol* 2005;131: 59–66.
38. Liu X, Wang B, Ma X, Guo Y. NF-kappaB activation through the alternative pathway correlates with chemoresistance and poor survival in extranodal NK/T-cell lymphoma, nasal type. *Jpn J Clin Oncol* 2009;39:418–24.
39. Chen S, Blank JL, Peters T, Liu XJ, Rappoli DM, Pickard MD, Menon S, Yu J, Driscoll DL, Lingaraj T, Burkhardt AL, Chen W,

et al. Genome-wide siRNA screen for modulators of cell death induced by proteasome inhibitor bortezomib. *Cancer Res* 2010;70:4318–26.
40. Nencioni A, Grunebach F, Patrone F, Ballestrero A, Brossart P. Proteasome inhibitors: antitumor effects and beyond. *Leukemia* 2007;21:30–6.
41. Cordova C, Munker R. The presence or absence of latent Epstein-Barr virus does not alter the sensitivity of Burkitt's lymphoma cell lines to proteasome inhibitors. *Acta Haematol* 2008;119:241–3.
42. Shair KH, Bendt KM, Edwards RH, Bedford EC, Nielsen JN, Raab-Traub N. EBV latent membrane protein 1 activates Akt, NFkappaB, and Stat3 in B cell lymphomas. *PLoS Pathog* 2007;3:e166.
43. Brown HJ, Song MJ, Deng H, Wu TT, Cheng G, Sun R. NF-kappaB inhibits gammaherpesvirus lytic replication. *J Virol* 2003;77:8532–40.
44. Ogawa Y, Tobinai K, Ogura M, Ando K, Tsuchiya T, Kobayashi Y, Watanabe T, Maruyama D, Morishima Y, Kagami Y, Taji H, Minami H, et al. Phase I and II pharmacokinetic and pharmacodynamic study of the proteasome inhibitor bortezomib in Japanese patients with relapsed or refractory multiple myeloma. *Cancer Sci* 2008;99:140–4.
45. Heider U, Rademacher J, Lamottke B, Mieth M, Moebs M, von Metzler I, Assaf C, Sezer O. Synergistic interaction of the histone deacetylase inhibitor SAHA with the proteasome inhibitor bortezomib in cutaneous T cell lymphoma. *Eur J Haematol* 2009;82:440–9.
46. Kawada J, Zou P, Mazitschek R, Bradner JE, Cohen JI. Tubacin kills Epstein-Barr virus (EBV)-Burkitt lymphoma cells by inducing reactive oxygen species and EBV lymphoblastoid cells by inducing apoptosis. *J Biol Chem* 2009;284:17102–9.
47. Stamatopoulos B, Meuleman N, De Bruyn C, Mineur P, Martiat P, Bron D, Lagneaux L. Antileukemic activity of valproic acid in chronic lymphocytic leukemia B cells defined by microarray analysis. *Leukemia* 2009;23:2281–9.
48. Yajima M, Imadome K, Nakagawa A, Watanabe S, Terashima K, Nakamura H, Ito M, Shimizu N, Honda M, Yamamoto N, Fujiwara S. A new humanized mouse model of Epstein-Barr virus infection that reproduces persistent infection, lymphoproliferative disorder, and cell-mediated and humoral immune responses. *J Infect Dis* 2008;198:673–82.
49. Hong GK, Gulley ML, Feng WH, Delecluse HJ, Holley-Guthrie E, Kenney SC. Epstein-Barr virus lytic infection contributes to lymphoproliferative disease in a SCID mouse model. *J Virol* 2005;79:13993–4003.
50. Strowig T, Gurer C, Ploss A, Liu YF, Arrey F, Sashihara J, Koo G, Rice CM, Young JW, Chadburn A, Cohen JI, Munz C. Priming of protective T cell responses against virus-induced tumors in mice with human immune system components. *J Exp Med* 2009;206:1423–34.

VOLUME 29 · NUMBER 33 · NOVEMBER 20 2011

JOURNAL OF CLINICAL ONCOLOGY

ORIGINAL REPORT

Phase II Study of SMILE Chemotherapy for Newly Diagnosed Stage IV, Relapsed, or Refractory Extranodal Natural Killer (NK)/T-Cell Lymphoma, Nasal Type: The NK-Cell Tumor Study Group Study

Motoko Yamaguchi, Yok-Lam Kwong, Won Seog Kim, Yoshinobu Maeda, Chizuko Hashimoto, Cheolwon Suh, Koji Izutsu, Fumihiro Ishida, Yasushi Isobe, Eisaburo Sueoka, Junji Suzumiya, Takao Kodama, Hiroshi Kimura, Rie Hyo, Shigeo Nakamura, Kazuo Oshimi, and Ritsuro Suzuki

Motoko Yamaguchi, Mie University Graduate School of Medicine, Tsu; Yoshinobu Maeda, Okayama University Graduate School of Medicine, Okayama; Chizuko Hashimoto, Kanagawa Cancer Center, Yokohama; Koji Izutsu, NTT Medical Center Tokyo; Yasushi Isobe and Kazuo Oshimi, Juntendo University School of Medicine, Tokyo; Fumihiro Ishida, Shinshu University School of Medicine, Matsumoto; Eisaburo Sueoka, Saga University School of Medicine, Saga; Junji Suzumiya, Fukuoka University Chikushi Hospital, Fukuoka; Takao Kodama, Miyazaki University School of Medicine, Miyazaki; Hiroshi Kimura, Rie Hyo, Shigeo Nakamura, and Ritsuro Suzuki, Nagoya University Graduate School of Medicine, Nagoya, Japan; Yok-Lam Kwong, Queen Mary Hospital, University of Hong Kong, Hong Kong, China; Won Seog Kim, Samsung Medical Center, Sungkyunkwan University School of Medicine; Cheolwon Suh, Asan Medical Center, University of Ulsan College of Medicine, Seoul, Korea; and Kazuo Oshimi, Eisai Research Institute of Boston, Andover, MA.

Submitted February 25, 2011; accepted July 28, 2011; published online ahead of print at www.jco.org on October 11, 2011.

Supported by a Grant-in-Aid for Cancer Research from the Ministry of Health, Labor and Welfare of Japan.

Authors' disclosures of potential conflicts of interest and author contributions are found at the end of this article.

Clinical Trials repository link available on JCO.org.

Corresponding author: Ritsuro Suzuki, MD, PhD, Department of HSCT Data Management & Biostatistics, Nagoya University, Graduate School of Medicine, 1-1-20 Daiko-Minami, Higashi-ku, Nagoya, 461-0047 Japan; e-mail: r-suzuki@med.nagoya-u.ac.jp.

0732-183X/11/2933-4410/$20.00

DOI: 10.1200/JCO.2011.35.6287

ABSTRACT

Purpose
To explore a more effective treatment for newly diagnosed stage IV, relapsed, or refractory extranodal natural killer/T-cell lymphoma, nasal type (ENKL), we conducted a phase II study of the steroid (dexamethasone), methotrexate, ifosfamide, L-asparaginase, and etoposide (SMILE) regimen.

Patients and Methods
Patients with newly diagnosed stage IV, relapsed, or refractory disease and a performance status of 0 to 2 were eligible. Two cycles of SMILE chemotherapy were administered as the protocol treatment. The primary end point was the overall response rate (ORR) after the protocol treatment.

Results
A total of 38 eligible patients were enrolled. The median age was 47 years (range, 16 to 67 years), and the male:female ratio was 21:17. The disease status was newly diagnosed stage IV in 20 patients, first relapse in 14 patients, and primary refractory in four patients. The eligibility was revised to include lymphocyte counts of 500/μL or more because the first two patients died from infections. No treatment-related deaths were observed after the revision. The ORR and complete response rate after two cycles of SMILE chemotherapy were 79% (90% CI, 65% to 89%) and 45%, respectively. In the 28 patients who completed the protocol treatment, 19 underwent hematopoietic stem-cell transplantation. The 1-year overall survival rate was 55% (95% CI, 38% to 69%). Grade 4 neutropenia was observed in 92% of the patients. The most common grade 3 or 4 nonhematologic complication was infection (61%).

Conclusion
SMILE chemotherapy is an effective treatment for newly diagnosed stage IV, relapsed or refractory ENKL. Myelosuppression and infection during the treatment should be carefully managed.

J Clin Oncol 29:4410-4416. © 2011 by American Society of Clinical Oncology

INTRODUCTION

Extranodal natural killer (NK)/T-cell lymphoma, nasal type (ENKL), is a lymphoma associated with the Epstein-Barr virus (EBV), which is much more common in Asia and Latin America than in Western countries.[1,2] More than two thirds of patients with ENKL have stage I or II disease in the upper aerodigestive tract.[3-6] The prognosis for localized ENKL has been improving as a result of the use of either concurrent chemoradiotherapy[7,8] or chemotherapy with sandwiched radiotherapy.[9] In contrast, most patients with newly diagnosed stage IV, relapsed, or refractory ENKL treated with conventional chemotherapy designed for aggressive lymphomas, such as cyclophosphamide, doxorubicin, vincristine, and prednisone, survive for less than a year.[6] The poor outcome is partly because ENKL tumor cells express P-glycoprotein, which results in tumor multidrug resistance.[10-12] There are a number of long-term survivors among patients with advanced-stage, relapsed, or refractory ENKL who have undergone hematopoietic stem-cell transplantation (HSCT).[13-15] However, patients who received HSCT in complete response (CR) showed better prognosis than those who received HSCT during non CR. Therefore, the development of an effective chemotherapy for these patients is an important initial step in improving treatment outcomes.

Table 1. SMILE Chemotherapy

Agent	Dose/d	Route	Day
Methotrexate	2 g/m^2*	IV (6 hours)	1
Leucovorin	15 mg × 4	IV or PO	2, 3, 4
Ifosfamide	1,500 mg/m^2	IV	2, 3, 4
Mesna	300 mg/m^2 × 3	IV	2, 3, 4
Dexamethasone	40 mg/d	IV or PO	2, 3, 4
Etoposide	100 mg/m^2*	IV	2, 3, 4
L-asparaginase (*Escherichia coli*)	6,000 U/m^2	IV	8, 10, 12, 14, 16, 18, 20
G-CSF		SC or IV	Day 6 to WBC > 5,000/μL

NOTE. Cycles were repeated every 28 days. Two courses were planned as the protocol treatment.
Abbreviations: G-CSF, granulocyte-colony stimulating factor; IV, intravenously; PO, orally; SC, subcutaneous injection; SMILE, steroid (dexamethasone), methotrexate, ifosfamide, L-asparaginase, and etoposide.
*The recommended dose was determined in the preceding phase I study.

To explore the possibility of more effective induction chemotherapy for NK-cell neoplasms, the NK-Cell Tumor Study Group, comprising Japanese and Asian hematologists, has formulated a novel chemotherapeutic regimen: steroid (dexamethasone), methotrexate, ifosfamide, L-asparaginase, and etoposide (SMILE). These agents are multidrug resistance independent and may be key drugs for NK-cell neoplasms or for EBV-associated disease. From the phase I trial of SMILE, the recommended doses of methotrexate and etoposide were determined.[16] The CR rate in the phase I trial was 50% (three of six eligible patients), and the overall response rate (ORR) was 67% (four of six patients). To further evaluate the efficacy of SMILE chemotherapy, we conducted a subsequent phase II study.

PATIENTS AND METHODS

Eligibility Criteria

Patients with newly diagnosed stage IV, relapsed, or refractory disease who had undergone first-line chemotherapy were eligible. Those with aggressive NK-cell leukemia were excluded because no patients with aggressive NK-cell leukemia had been enrolled in the prior phase I study.[16] Patients who had received autologous HSCT more than 12 months before registration were also eligible. The other inclusion and exclusion criteria for the study were the same as those for the prior phase I study.[16] Briefly, patients from 15 to 69 years of age with a performance status of 0 to 2, based on the Eastern Cooperative Oncology Group scale, and preserved organ functions were included. Neither chemotherapy nor radiotherapy was administered within 21 days before registration. Patients who had clinical symptoms of CNS involvement were excluded.

The pretreatment staging procedures included a physical examination, a bone marrow aspiration and/or biopsy, a chest radiograph, and a computed tomography scan of the nasal cavity, neck, chest, abdomen, and pelvis. An endoscopy of the upper gastrointestinal tract and a positron emission tomography scan were recommended but not mandatory.

After patient enrollment, hematoxylin-eosin–stained sections were histologically reviewed by the Central Pathology Review Board based on the WHO classification.[1] Immunohistochemical staining was performed at the central pathology office using formalin-fixed, paraffin-embedded sections with antibodies against CD3, CD20, CD56, perforin, and granzyme B. In addition, in situ hybridization for EBV-encoded small RNA-1 was performed.

Registration of patients was conducted by facsimile between the participating physicians and the Center for Supporting Hematology-Oncology Trials Data Center (Nagoya, Japan). The study was approved by both the protocol review committee and the institutional review board of each institution. Written informed consent was obtained from all of the patients. The study was registered to the University Hospital Medical Information Network Clinical Trials Registry.

Treatment

SMILE chemotherapy was administrated as indicated in Table 1. On the basis of the results of the phase I trial,[16] administration of granulocyte colony-stimulating factor was mandatory from day 6 and discontinued if the leukocyte count exceeded 5,000/μL after the nadir phase. Antibiotic prophylaxis of sulfamethoxazole-trimethoprim was recommended. The criteria for the initiation of a second course of SMILE were as follows (1): a total of 4 weeks or more had passed since the prior course; (2) all of the following were achieved at least 1 day before the second course of SMILE: a leukocyte count of $\geq$ 2,000/μL, a platelet count of $\geq$ 100,000/μL, AST and ALT levels $\leq$ 5× the upper limit of normal, total bilirubin of $\leq$ 2.0 mg/dL, or serum creatinine of $\leq$ 1.5 mg/dL; and (3) there were no other symptoms or complications that were not suitable for the initiation of a second course. If there was no recovery 4 weeks after the day of the scheduled second course, the protocol treatment was terminated. Two courses of SMILE chemotherapy were planned for the protocol treatment. After the planned two courses, patients could undergo additional courses of SMILE and/or other chemotherapy, with or without autologous/allogeneic HSCT. The decision was made according to the discretion of treating physicians mainly on the basis of the patient's age, conditions, and the availability of HSC donors.

Response and Toxicity Criteria

The responses were assessed by the Central Imaging Review Board according to criteria modified from the WHO response criteria[17] that were also used in the prior phase I study of SMILE chemotherapy.[16] All of the examinations for restaging were done within 4 to 6 weeks (from day 22 to day 42) of the second course of SMILE. Because ENKL frequently occurs in the nasal/paranasal sites and leaves scar or necrotic tissue, it is sometimes difficult to determine whether or not a patient strictly attains CR using the WHO response criteria[17] or the International Workshop criteria.[18] Therefore, in this trial, CR was defined as the complete disappearance of all objective signs of disease, including enlarged lymph nodes or hepatomegaly and splenomegaly at the restaging. Partial response (PR) was defined as at least a 50% reduction of tumor volume without the occurrence of new lesions at the restaging. Progressive disease was defined as a greater than 25% increase in the sum of tumor lesions or the emergence of one or more new lesion(s) or clinical symptoms that indicate disease progression, such as "B" symptoms or elevated serum lactate dehydrogenase levels. No response was defined as any response that did not fall into the other defined categories. If a patient died before day 42 of the second course of SMILE and could not undergo the defined restaging procedure, the patient's response was recorded as early death. The ORR rate was defined as the proportion of all patients who were able to be evaluated for response who experienced CR or PR.

Toxicity was graded according to the Common Terminology Criteria for Adverse Events (CTCAE) version 3.0. In cases of grade 4 thrombocytopenia,

doses of methotrexate, ifosfamide, and etoposide were reduced to two thirds of their previous levels in the second course. L-asparaginase was discontinued if it induced grades 3 or 4 allergic reactions/hypersensitivity, pancreatitis, or hypotension. If L-asparaginase induced grades 1 or 2 allergic reactions/hypersensitivity, the dose of L-asparaginase was reduced by half. In this case, the use of prednisone at a dose of 1 mg/kg/d was permitted. L-asparaginase was stopped if grade 4 thrombocytopenia or grade 3 nonhematologic toxicity was observed. In the cases for which the first course of L-asparaginase was discontinued, L-asparaginase was readministered if the patient recovered from grade 4 thrombocytopenia or grade 3 nonhematologic toxicity. If the concentration of methotrexate exceeded 1×10^{-7} mol/L 72 hours after the administration during the first course, the dose of methotrexate in the second course was reduced to two thirds.

Statistical Analysis

The primary end point was an ORR after two courses of SMILE chemotherapy. The secondary end points were CR rate after two courses of SMILE chemotherapy, 1-year overall survival (OS), response of the subgroup, or toxicity. The expected ORR was estimated to be 60%, and the threshold ORR was estimated to be 35%, on the basis of our previous observations.[6,19] With a statistical power of 80% and a one-sided, type I error of 5%, the number of eligible patients required for this study was calculated to be 25 using a binomial analysis method. The projected sample size was 28 patients, with an accrual of 3 years and the expectation that 10% of patients would be deemed ineligible.

OS was defined as the time from registration until death from any cause or until the date of the last follow-up for the patients who survived. Survival estimates were calculated using the Kaplan-Meier method, and the hazard ratio (HR) was estimated using a Cox regression. All analyses were performed using STATA SE 10 software (STATA, College Station, TX).

RESULTS

Patient Characteristics

As a result of an excellent accrual, the study protocol was revised to increase the statistical power from 80% to 90% in March 2009. The projected number of patients for this study was increased from 28 to 38. Ultimately, 39 patients were enrolled from 19 institutions between July 2007 and October 2009. Histologic diagnosis of all patients except one was confirmed as ENKL by the Central Pathology Review Board. The single patient who was excluded from further analyses was judged to have CD56-positive rhabdomyosarcoma by the Central Pathology Review Board.

The baseline characteristics of 38 eligible patients are listed in Table 2. The median age was 47 years (range, 16 to 67 years), and the male:female ratio was 21:17. Twenty patients (53%) had newly diagnosed stage IV disease, 14 were in first relapse, and four were in primary refractory state. Two patients were treated with radiation alone as the initial therapy. Among the 16 patients who received chemotherapy as their first-line therapy, five patients were treated with anthracycline-containing chemotherapies, and 13 patients were treated with platinum-based regimens. Two patients were treated with chemotherapy containing both anthracycline and platinum.

Table 2. Baseline Patient Characteristics (N = 38)

Characteristic	No. of Patients	%
Age, years		
Median	47	
Range	16 to 67	
Sex		
Male	21	55
Female	17	45
Site(s) of involvement at diagnosis		
Upper aerodigestive tract	35	92
Extra-upper aerodigestive tract only	3	8
Disease state		
Newly diagnosed stage IV	20	53
First relapse	14	37
Refractory to the first-line treatment	4	11
Stage at enrollment		
IE or IIE	11	29
IIIE or IV	27	71
"B" symptoms present	18	47
Elevated serum LDH	16	42
Performance status		
0	21	55
1	12	32
2	5	13
Prior treatment		
None	20	53
Radiotherapy alone	2	5
Chemotherapy alone	3	8
Concurrent chemoradiotherapy	9	24
RT-DeVIC	6	
CCRT-VIPD or VIDL	2	
RT-CHOP	1	
Other combined modality therapies	4	11

Abbreviations: CCRT, concurrent chemoradiotherapy; DeVIC, dexamethasone, etoposide, ifosfamide, and carboplatin; LDH, lactate dehydrogenase; VIDL, etoposide, ifosfamide, dexamethasone, and L-asparaginase; VIPD, etoposide, ifosfamide, cisplatin, and dexamethasone.

Treatment

Twenty-eight patients (74%) completed the planned treatment. In two patients, the treatment was discontinued on day 4 because of methotrexate-associated encephalopathy and intestinal perforation owing to rapid tumor lysis. L-asparaginase was discontinued in four patients due to adverse events (AEs), including two patients with allergy to L-asparaginase (both in the second course), one patient with pancreatitis (grade 2, in the first course), and one patient with liver function derangement (in the first course). In two of these four patients, L-asparaginase was readministered at a 50% dose reduction. One allergic patient received simultaneously prednisolone 1 mg/kg. In another four patients, L-asparaginase was also stopped per protocol, owing to AEs of preceding agents (methotrexate, ifosfamide, and etoposide), including two patients with infections and two patients with thrombocytopenia. The relative dose-intensity of L-asparaginase in the first course of SMILE was 81%. Two of these eight patients who had L-asparaginase discontinued achieved CR. The relative dose-intensity of CR patients was 92%.

Additional courses of SMILE were given for 21 patients (one course, 10 patients; two courses, three patients; three courses, two patients; four courses, six patients). The median number of courses of SMILE administered was three (range, one to six courses). Treatment of the 28 patients who completed two courses of SMILE were as follows: chemotherapy only (n = 7), autologous HSCT (n = 4), or allogeneic HSCT (n = 17; myeloablative, n = 15, nonmyeloablative, n = 2). No difficulties in mobilizing peripheral blood HSC were encountered in the four patients who received autologous HSCT. Among the seven patients who did not complete the protocol treatment, two of them received no additional treatment and died as a

Table 3. Incidence and Maximum Severity of Adverse Events (N = 38)

Adverse Event	Grade 3		Grade 4	
	No.	%	No.	%
Hematologic				
Leukopenia	9	24	29	76
Neutropenia	3	8	35	92
Anemia	18	47	1	3
Thrombocytopenia	9	24	15	40
Nonhematologic				
Hypofibrinogenemia	4	11	0	0
APTT elongation	4	11	0	0
Hypoalbuminemia	6	16	0	0
Hyperbilirubinemia	3	8	1	3
AST elevation	12	32	0	0
ALT elevation	10	26	2	6
Creatinine	2	5	0	0
Hyponatremia	11	29	1*	3
Hyperglycemia	7	18	0	0
Amylase	6	16	1*	3
Appetite loss	8	21	1*	3
Diarrhea	4	11	0	0
Nausea	5	13	0	0
Mucositis	5	13	0	0
Vomiting	2	5	0	0
Infection	17	45	6†	16
Somnolence	1	3	2	5
Encephalopathy	0	0	1	3

NOTE. Grade 3 hypernatremia, allergic reaction, fever, and dehydration were observed in one patient each.
Abbreviation: APTT, activated partial thromboplastin time.
*Related to grade 2 pancreatitis in one patient.
†Including the two patients who died as a result of infection (two treatment-related deaths).

Table 4. Response After Two Cycles of SMILE Chemotherapy (N = 38)

Response	All Patients (N = 38)		Newly Diagnosed Stage IV (n = 20)		First Relapse (n = 14)		Refractory to the First-Line Therapy (n = 4)	
	No.	%	No.	%	No.	%	No.	%
CR	17	45	8	40	9	64	0	0
PR	13	34	8	40	4	29	1	25
NR	1	3	1	5	0	0	0	0
PD	4	10	1	5	1	7	2	50
ED	3	8	2	10	0	0	1	25

Abbreviations: CR, complete response; ED, early death; NR, no response; PD, progressive disease; PR, partial response; SMILE, steroid (dexamethasone), methotrexate, ifosfamide, L-asparaginase, and etoposide.

result of disease. Three patients were treated with other chemotherapy, and two of them underwent allogeneic HSCT without response.

Toxicity

Table 3 lists all grade 3 or 4 AEs that occurred in the 38 eligible patients who were enrolled onto this trial. After the death of initial two patients from grade 5 infections (patients 1 and 2; see Appendix, online only), the protocol was revised to include a careful assessment of infection and the incorporation of a lymphocyte count of $\geq 500/\mu L$ into the eligibility criteria. There were no subsequent treatment-related deaths.

Grade 4 neutropenia was common (92%). The nonhematologic grade 4 toxicities included infection (n = 6), hyperbilirubinemia (n = 1), ALT elevation (n = 2), and encephalopathy (n = 1); two patients experienced grade 4 somnolence, which was complicated by a grade 3 infection in one patient and by grade 4 encephalopathy in the other patient. One patient experienced grade 2 pancreatitis and had complications from grade 4 hyponatremia, hyperamylasemia, and appetite loss. The most common grade 3 nonhematologic AE was infection (45%). Allergic reactions due to L-asparaginase of any grade were observed in five patients (three with grade 1, one with grade 2, and one with grade 3). The toxic profiles according to disease status at the time of study entry (newly diagnosed/relapsed/refractory) are shown in Appendix Table A1 (online only). The grade 4 hematologic toxicity rates of newly diagnosed and relapsed patients were 95% and 93%, respectively. The grade 4 nonhematologic toxicity rates of newly diagnosed and relapsed patients were 35% and 14%, respectively. None of these differences were statistically significant ($P = .99$ and $P = .25$). No clinical predictors of toxicity were found. Only hyponatremia was associated with newly diagnosed and refractory diseases.

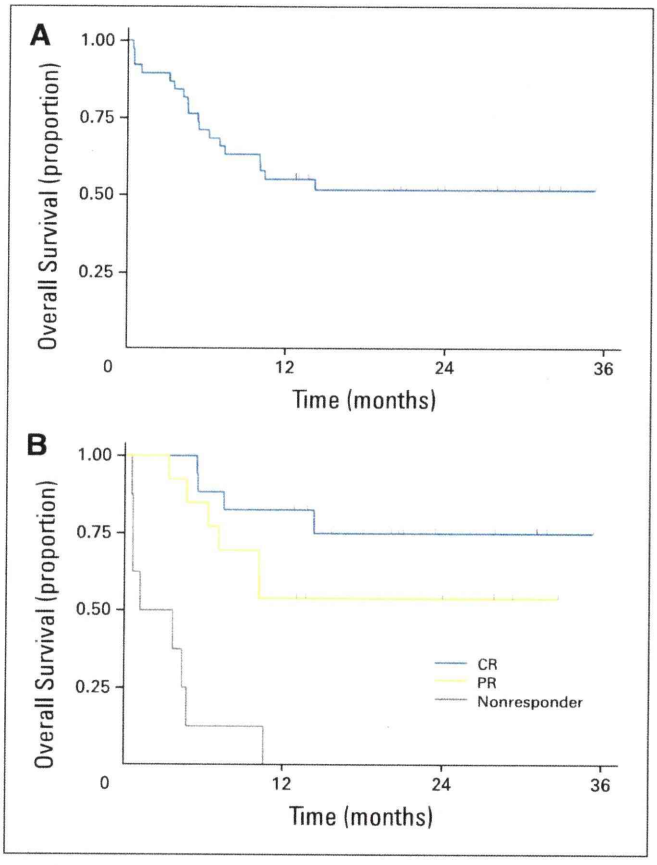

Fig 1. Kaplan-Meier estimates of overall survival (OS) of patients treated with steroid (dexamethasone), methotrexate, ifosfamide, L-asparaginase, and etoposide chemotherapy. (A) The 1-year OS of 38 patients was 55% (95% CI, 38% to 69%). The median follow-up of survivors was 24 months (range, 13 to 35 months). (B) The 1-year OS was 82% (95% CI, 55% to 94%) for patients who attained complete response (CR) and 54% (95% CI, 25% to 76%) for those who attained partial response (PR).

Efficacy and Survival

Among the 38 eligible patients, the response was CR in 17 patients (45%), PR in 13 patients, no response in one patient, progressive disease in four patients, and early death in three patients (Table 4). The ORR was 79% (90% CI, 65% to 89%). There were no differences in either the ORR or CR rate between patients with newly diagnosed stage IV disease and those with first-relapse disease. With respect to progressive disease in four patients, one occurred during the first course of SMILE, one after the first course, and two after the completion of two courses.

The median follow-up time of the living patients was 24 months, with a range of 13 to 35 months. The OS rate at 1 year, which was one of the secondary end points, was 55% (95% CI, 38% to 69%; Fig 1A). The progression-free survival (PFS) at 1 year was 53% (95% CI, 36% to 67%). The patients who attained response with SMILE chemotherapy had a higher OS (Fig 1B). The OS and PFS by the disease state at entry are shown in Figure 2A and 2B. Patients with relapsed disease showed better 1-year OS (79%) and PFS (71%) as compared with patients with refractory disease (P = .04 and .05, respectively). The survival curves of patients (excluding early deaths; n = 35) according to the type of poststudy therapy (autologous/allogeneic HSCT/chemotherapy) are shown in Figures 2C and 2D. Patients who received autologous HSCT seemed to show better OS and PFS, but the difference was not statistically significant. Univariate analysis for OS showed that presence of B symptoms (HR, 3.1, P = .01), performance status of 1 or 2 (HR, 3.1, P = .002), elevated serum lactate dehydrogenase (HR, 6.1, P = .001), and hemoglobin of less than 12 g/dL (HR, 3.9, P = .007) were significant prognostic factors.

DISCUSSION

Our results indicate that SMILE chemotherapy is effective for the treatment of newly diagnosed stage IV, relapsed, or refractory ENKL. The ORR after two cycles of SMILE (79%; 90% CI, 65% to 89%) clearly exceeded the threshold ORR (35%).[20] The 1-year OS rate (55%) was much improved compared with the previous treatment strategy.

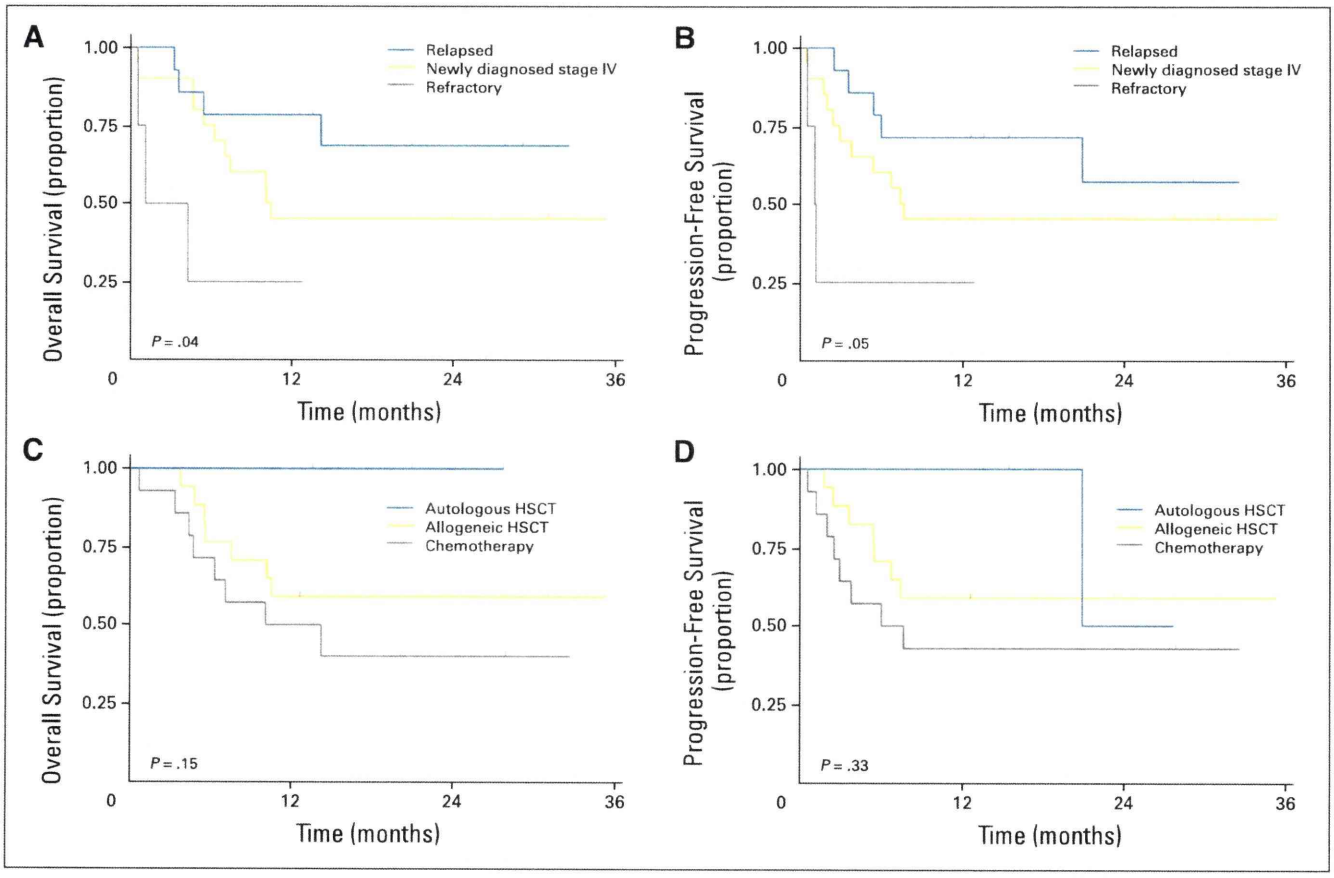

Fig 2. Kaplan-Meier estimates of overall survival (OS) and progression-free survival (PFS) of patients by the subgroup analysis. (A) OS of patients by the disease state at entry. The 1-year OS was 45% (95% CI, 23% to 65%) for patients with newly diagnosed stage IV disease, 79% (95% CI, 47% to 93%) for patients with relapsed disease, and 25% (95% CI, 1% to 67%) for patients with refractory disease. The difference was statistically significant (P = .04). (B) PFS of patients by the disease state at entry. The 1-year PFS was 45% (95% CI, 23% to 65%) for patients with newly diagnosed stage IV disease, 71% (95% CI, 41% to 88%) for patients with relapsed disease, and 25% (95% CI, 1% to 67%) for patients with refractory disease. The difference was statistically significant (P = .05). (C) OS of patients excluding early death (n = 35) by type of poststudy therapy. The 1-year OS was 100% for patients who received autologous hematopoietic stem-cell transplantation (HSCT), 59% (95% CI, 36% to 78%) for patients who received allogeneic HSCT, and 41% (95% CI, 19% to 63%) for patients treated with chemotherapy only. The difference was not statistically significant (P = .15). (D) PFS of patients excluding early death by type of poststudy therapy. The 1-year PFS was 100% for patients who received autologous HSCT, 59% (95% CI, 36% to 78%) for patients who received allogeneic HSCT, and 35% (95% CI, 14% to 57%) for patients treated with chemotherapy only. The difference was not statistically significant (P = .33).

With regard to the safety of SMILE, myelosuppression and infection should be carefully monitored during and after SMILE chemotherapy. To avoid severe AEs, the use of granulocyte colony-stimulating factor is considered mandatory, starting on day 6 and continuing until recovery beyond the nadir. In addition, full-dose administration of SMILE should be avoided for patients who are in poor condition, including those with lymphopenia less than 500/μL or large tumor burden. A lymphocyte count was added to the eligibility criteria because all three of the patients who died of neutropenic infection in the phase I and phase II SMILE studies had low lymphocyte counts before treatment. Decreased-dose SMILE[21] and less-intensive L-asparaginase chemotherapies[22-24] are candidate strategies for those patients with poor pretreatment conditions.

L-asparaginase–based chemotherapy has been highlighted as a promising treatment for ENKL. L-asparaginase was shown to induce apoptosis of ENKL cells in vitro; this result was attributed to low asparagine synthetase expression.[25] In fact, there were several case reports in the early 2000s in which ENKL showed an excellent response to L-asparaginase.[26-30] Recently, a phase II study of L-asparaginase, methotrexate, and dexamethasone (AspaMetDex) for relapsed or refractory ENKL was reported by a French group.[22] Nineteen patients were enrolled, and the CR rate was 61%. The median survival time was 12.2 months, and the 1-year OS was 45%. The AspaMetDex therapy is also promising, but there are several differences from the SMILE study. First, 53% of patients in our SMILE study had newly diagnosed stage IV ENKL which showed poor prognosis with conventional chemotherapy.[6] In contrast, the GELA (Groupe d'Etude des Lymphomes de l'Adulte)/GOELAMS (Groupe Ouest-Est des Leucémies et des Autres Maladies du Sang) study included only patients with relapsed/refractory disease. This resulted in a different ratio of patients with advanced-stage disease between the SMILE study (27 of 38 patients, 71%) and the AspaMetDex study (seven of 19 patients, 37%). Second, 17 of the 19 patients were initially treated with anthracycline-based chemotherapy in the French study. In contrast, 81% of the patients who had prior therapy in our study received platinum-based chemotherapy before SMILE, which suggests that different patient groups were selected in the two studies. Currently, these SMILE and AspaMetDex regimens are both promising for relapsed/refractory ENKL. A comparative study is required for a conclusion, but is not realistic for this type of rare lymphoma.

The optimal course of SMILE chemotherapy and the most appropriate timing of HSCT for patients after two courses of SMILE remain undetermined. In addition, the optimal treatment strategy for patients who cannot undergo HSCT needs further clinical evaluation. It has been speculated that the SMILE regimen may also be effective for T-cell lymphomas because ENKL and mature T-cell lymphomas share several clinical and pathologic features, such as extranodal predilection and expression of cytotoxic molecules. This speculation should be confirmed in further clinical studies.

In conclusion, the results of this phase II study demonstrate that two cycles of SMILE is an effective chemotherapy regimen for patients with newly diagnosed stage IV, relapsed, or refractory ENKL. However, the SMILE regimen is potentially toxic, and careful patient monitoring is needed.

AUTHORS' DISCLOSURES OF POTENTIAL CONFLICTS OF INTEREST

Although all authors completed the disclosure declaration, the following author(s) indicated a financial or other interest that is relevant to the subject matter under consideration in this article. Certain relationships marked with a "U" are those for which no compensation was received; those relationships marked with a "C" were compensated. For a detailed description of the disclosure categories, or for more information about ASCO's conflict of interest policy, please refer to the Author Disclosure Declaration and the Disclosures of Potential Conflicts of Interest section in Information for Contributors.

Employment or Leadership Position: Kazuo Oshimi, Eisai Pharmaceutical (C) **Consultant or Advisory Role:** None **Stock Ownership:** None **Honoraria:** Ritsuro Suzuki, Kyowa-Hakko Kirin **Research Funding:** None **Expert Testimony:** None **Other Remuneration:** None

AUTHOR CONTRIBUTIONS

Conception and design: Motoko Yamaguchi, Junji Suzumiya, Kazuo Oshimi, Ritsuro Suzuki
Administrative support: Ritsuro Suzuki
Provision of study materials or patients: Yok-Lam Kwong, Won Seog Kim, Yoshinobu Maeda, Chizuko Hashimoto, Cheolwon Suh, Koji Izutsu, Fumihiro Ishida, Yasushi Isobe, Eisaburo Sueoka
Collection and assembly of data: Motoko Yamaguchi, Yok-Lam Kwong, Won Seog Kim, Yoshinobu Maeda, Chizuko Hashimoto, Cheolwon Suh, Koji Izutsu, Fumihiro Ishida, Yasushi Isobe, Eisaburo Sueoka, Rie Hyo, Ritsuro Suzuki
Data analysis and interpretation: Motoko Yamaguchi, Takao Kodama, Hiroshi Kimura, Rie Hyo, Shigeo Nakamura, Kazuo Oshimi, Ritsuro Suzuki
Manuscript writing: All authors
Final approval of manuscript: All authors

REFERENCES

1. Chan JKC, Jaffe ES, Ralfkiaer E: Extranodal NK/T-cell lymphoma, nasal type, in Jaffe ES, Harris NL, Stein H (eds): World Health Organization Classification of Tumors: Pathology and Genetics of Tumours of Haematopoietic and Lymphoid Tissues. Lyon, France, IARC Press, 2001, pp 204-207

2. Chan JKC, Quintanilla-Martinez L, Ferry JA: Extranodal NK/T-cell lymphoma, nasal type, in Swerdlow SH, Campo E, Harris NL (eds): WHO Classification of Tumours of Haematopoietic and Lymphoid Tissues. Lyon, France, International Agency for Research on Cancer, 2008, pp 285-288

3. Lee J, Suh C, Park YH, et al: Extranodal natural killer T-cell lymphoma, nasal-type: A prognostic model from a retrospective multicenter study. J Clin Oncol 24:612-618, 2006

4. Kim TM, Lee SY, Jeon YK, et al: Clinical heterogeneity of extranodal NK/T-cell lymphoma, nasal type: A national survey of the Korean Cancer Study Group. Ann Oncol 19:1477-1484, 2008

5. Au WY, Weisenburger DD, Intragumtornchai T, et al: Clinical differences between nasal and extranasal natural killer/T-cell lymphoma: A study of 136 cases from the International Peripheral T-Cell Lymphoma Project. Blood 113:3931-3937, 2009

6. Suzuki R, Suzumiya J, Yamaguchi M, et al: Prognostic factors for mature natural killer (NK) cell neoplasms: Aggressive NK cell leukemia and extranodal NK cell lymphoma, nasal type. Ann Oncol 21:1032-1040, 2010

7. Yamaguchi M, Tobinai K, Oguchi M, et al: Phase I/II study of concurrent chemoradiotherapy for localized nasal natural killer/T-cell lymphoma: Japan Clinical Oncology Group Study JCOG0211. J Clin Oncol 27:5594-5600, 2009

8. Kim SJ, Kim K, Kim BS, et al: Phase II trial of concurrent radiation and weekly cisplatin followed by VIPD chemotherapy in newly diagnosed, stage IE to IIE, nasal, extranodal NK/T-Cell Lymphoma: Consortium for Improving Survival of Lymphoma study. J Clin Oncol 27:6027-6032, 2009

9. Kwong YL, Anderson BO, Advani R, et al: Management of T-cell and natural-killer-cell neoplasms in Asia: Consensus statement from the

Asian Oncology Summit 2009. Lancet Oncol 10: 1093-1101, 2009

10. Yamaguchi M, Kita K, Miwa H, et al: Frequent expression of P-glycoprotein/MDR1 by nasal T-cell lymphoma cells. Cancer 76:2351-2356, 1995

11. Egashira M, Kawamata N, Sugimoto K, et al: P-glycoprotein expression on normal and abnormally expanded natural killer cells and inhibition of P-glycoprotein function by cyclosporin A and its analogue, PSC833. Blood 93:599-606, 1999

12. Drénou B, Lamy T, Amiot L, et al: CD3-CD56+ non-Hodgkin's lymphomas with an aggressive behavior related to multidrug resistance. Blood 89:2966-2974, 1997

13. Murashige N, Kami M, Kishi Y, et al: Allogeneic haematopoietic stem cell transplantation as a promising treatment for natural killer-cell neoplasms. Br J Haematol 130:561-567, 2005

14. Suzuki R, Suzumiya J, Nakamura S, et al: Hematopoietic stem cell transplantation for natural killer-cell lineage neoplasms. Bone Marrow Transplant 37:425-431, 2006

15. Kwong YL: High-dose chemotherapy and hematopoietic SCT in the management of natural killer-cell malignancies. Bone Marrow Transplant 44:709-714, 2009

16. Yamaguchi M, Suzuki R, Kwong YL, et al: Phase I study of dexamethasone, methotrexate, ifosfamide, L-asparaginase, and etoposide (SMILE) chemotherapy for advanced-stage, relapsed or refractory extranodal natural killer (NK)/T-cell lymphoma and leukemia. Cancer Sci 99:1016-1020, 2008

17. World Health Organization: WHO Handbook for Reporting Results of Cancer Treatment. Geneva, Switzerland, World Health Organization, 1979

18. Cheson BD, Horning SJ, Coiffier B, et al: Report of an international workshop to standardize response criteria for non-Hodgkin's lymphomas. J Clin Oncol 17:1244-1253, 1999

19. Oshimi K, Kawa K, Nakamura S, et al: NK-cell neoplasms in Japan. Hematology 10:237-245, 2005

20. Kim GE, Cho JH, Yang WI, et al: Angiocentric lymphoma of the head and neck: Patterns of systemic failure after radiation treatment. J Clin Oncol 18:54-63, 2000

21. Suzuki R: Treatment of advanced extranodal NK/T cell lymphoma, nasal-type and aggressive NK-cell leukemia. Int J Hematol 92:697-701, 2010

22. Jaccard A, Gachard N, Marin B, et al: Efficacy of L-asparaginase with methotrexate and dexamethasone (AspaMetDex regimen) in patients with refractory or relapsing extranodal NK/T-cell lymphoma, a phase II study. Blood 117:1834-1839, 2011

23. Yong W, Zheng W, Zhu J, et al: L-asparaginase in the treatment of refractory and relapsed extranodal NK/T-cell lymphoma, nasal type. Ann Hematol 88:647-652, 2009

24. Tsukune Y, Isobe Y, Yasuda H, et al: Activity and safety of combination chemotherapy with methotrexate, ifosfamide, l-asparaginase and dexamethasone (MILD) for refractory lymphoid malignancies: A pilot study. Eur J Haematol 84:310-315, 2010

25. Ando M, Sugimoto K, Kitoh T, et al: Selective apoptosis of natural killer-cell tumours by l-asparaginase. Br J Haematol 130:860-868, 2005

26. Rodriguez J, Romaguera JE, Manning J, et al: Nasal-type T/NK lymphomas: A clinicopathologic study of 13 cases. Leuk Lymphoma 39:139-144, 2000

27. Nagafuji K, Fujisaki T, Arima F, et al: L-asparaginase induced durable remission of relapsed nasal NK/T-cell lymphoma after autologous peripheral blood stem cell transplantation. Int J Hematol 74:447-450, 2001

28. Obama K, Tara M, Niina K: L-asparaginase-based induction therapy for advanced extranodal NK/T-cell lymphoma. Int J Hematol 78:248-250, 2003

29. Matsumoto Y, Nomura K, Kanda-Akano Y, et al: Successful treatment with Erwinia L-asparaginase for recurrent natural killer/T cell lymphoma. Leuk Lymphoma 44:879-882, 2003

30. Yong W, Zheng W, Zhang Y, et al: L-asparaginase-based regimen in the treatment of refractory midline nasal/nasal-type T/NK-cell lymphoma. Int J Hematol 78:163-167, 2003

Journal of General Virology (2011), **92**, 2590–2595 DOI 10.1099/vir.0.033712-0

Short Communication

Identification of Epstein–Barr virus-infected CD27$^+$ memory B-cells in liver or stem cell transplant patients

Yoshinori Ito,[1] Shinji Kawabe,[1] Seiji Kojima,[1] Fumihiko Nakamura,[2] Yukihiro Nishiyama,[3] Kenichiro Kaneko,[4] Tetsuya Kiuchi,[5] Hisami Ando[4] and Hiroshi Kimura[2]

Correspondence
Yoshinori Ito
yoshi-i@med.nagoya-u.ac.jp

[1]Department of Pediatrics, Nagoya University Graduate School of Medicine, Nagoya, Japan
[2]Department of Hematology and Oncology, Tenri Hospital, Tenri, Japan
[3]Department of Virology, Nagoya University Graduate School of Medicine, Nagoya, Japan
[4]Department of Pediatric Surgery, Nagoya University Graduate School of Medicine, Nagoya, Japan
[5]Department of Transplant Surgery, Nagoya University Graduate School of Medicine, Nagoya, Japan

To analyse the phenotype of Epstein–Barr virus (EBV)-infected lymphocytes in EBV-associated infections, cells from eight haematopoietic stem cell/liver transplantation recipients with elevated EBV viral loads were examined by a novel quantitative assay designed to identify EBV-infected cells by using a flow cytometric detection of fluorescent *in situ* hybridization (FISH) assay. By this assay, 0.05–0.78 % of peripheral blood lymphocytes tested positive for EBV, and the EBV-infected cells were CD20$^+$ B-cells in all eight patients. Of the CD20$^+$ EBV-infected lymphocytes, 48–83 % of cells tested IgD positive and 49–100 % of cells tested CD27 positive. Additionally, the number of EBV-infected cells assayed by using FISH was significantly correlated with the EBV-DNA load, as determined by real-time PCR (r^2=0.88, P<0.0001). The FISH assay enabled us to characterize EBV-infected cells and perform a quantitative analysis in patients with EBV infection after stem cell/liver transplantation.

Received 8 June 2011
Accepted 29 July 2011

Epstein–Barr virus (EBV) is a ubiquitous virus that infects humans worldwide. Acute infectious mononucleosis (AIM) is the primary EBV infection (Rickinson & Kieff, 2006), and current understanding of primary EBV infection is primarily based on studies of patients with AIM. EBV infects naïve B-cells in the tonsils and activates them; these infected B-cells can differentiate through a germinal centre in lymphoid tissue, becoming resting memory B-cells (Thorley-Lawson & Gross, 2004). Alternatively, EBV may infect memory cells directly (Kurth *et al.*, 2000).

EBV-related post-transplant lymphoproliferative disorder (PTLD) is a life-threatening disease following haematopoietic stem cell or solid organ transplantation, and EBV infects B-lymphocytes in most cases (Rickinson & Kieff, 2006). EBV also causes mild/moderate symptomatic diseases other than PTLD. Recently, serial EBV load monitoring following solid organ transplantation identified a population of recipients who subsequently developed and maintained very high EBV loads in the absence of clinical symptoms (Bingler *et al.*, 2008; D'Antiga *et al.*, 2007; Green *et al.*, 2009). In these cases, EBV also infected B-cells in peripheral blood (Gotoh *et al.*, 2010). Characterizing the EBV-infected lymphocytes in these different EBV-associated infections may provide a better understanding of the pathophysiology of EBV-related disorders.

We recently established a novel quantitative assay to identify EBV-infected cells that uses flow cytometric detection of fluorescent *in situ* hybridization (FISH) (Kimura *et al.*, 2009). With a fluorescein-conjugated probe that specifically hybridizes to the EBV-encoded small RNA (EBER), both nuclear EBER and surface lymphocyte antigens can be stained. This assay can be used with peripheral blood to characterize EBV-infected lymphocytes. With this FISH assay, we analysed peripheral blood in patients with EBV-associated T/NK-cell lymphoproliferative disease. The EBER-positive cells were found to be CD3$^+$CD4$^-$CD8$^-$TCR$\gamma\delta^+$ T-cells in patients with hydroa vacciniforme-like lymphoproliferative disease, which is an EBV-positive cutaneous T-cell lymphoma (Kimura *et al.*, 2009), thus providing new insight into EBV-associated T/NK-cell lymphoproliferative disease.

In this study, we applied the FISH assay to peripheral blood from eight haematopoietic stem cell/liver transplantation recipients with increasing amounts of EBV DNA in their peripheral blood to characterize the EBV-infected lymphocytes. The number of EBER-positive cells in peripheral

blood, as quantified by the FISH assay, was also compared with the EBV-DNA load, as determined by quantitative PCR.

Four haematopoietic stem cell transplant recipients and four liver transplant recipients were enrolled in the study. A quantitative PCR assay detected a large amount of EBV DNA in the peripheral blood of all of the patients. A prospective analysis of EBV load in peripheral blood is routinely performed in our department to provide an early diagnosis of EBV-associated diseases in patients after stem cell and liver transplantation. Blood samples for the FISH assay (described below) were obtained from: four haematopoietic stem cell transplantation recipients with suspected symptomatic EBV infection; four liver transplant recipients without clinical symptoms but with the continuous presence of high EBV viral loads; and five healthy volunteers with a history of EBV infection. PBMCs were separated by density gradients from whole blood. Informed consent was obtained from all participants or their parents. This study was approved by the University of Nagoya Institutional Review Board.

Viral load was examined in the PBMCs of all patients. Viral DNA was extracted from 1×10^6 PBMCs by using QIAamp DNA blood kits (Qiagen). The real-time quantitative PCR assay was performed as previously described (Kimura *et al.*, 1999; Wada *et al.*, 2007). The FISH assay was also performed as previously described (Kimura *et al.*, 2009). Briefly, for surface marker staining, 5×10^5 PBMCs were stained with phycoerythrin cyanin 5 (PC5)-labelled anti-CD20 mAb (clone B-Ly1, DakoCytomation), and phycoerythrin (PE)-labelled anti-IgD mAb (clone IgD26, MACS) or biotin-labelled anti-CD27 (clone O323, Biolegend) mAb, followed by streptavidin–PC5 (eBioscience), for 1 h at 4 °C. The cells were then fixed with 1 % acetic acid in 4 % paraformaldehyde/PBS (pH 7.4) for 40 min at 4 °C. After washing, cells were permeabilized in 50 µl 0.5 % Tween 20/PBS at room temperature. The cells were resuspended in 45 µl of hybridization solution (6 % dextran sulphate, 10 mM NaCl, 17.5 % formamide, 0.061 % sodium pyrophosphate, 0.12 % polyvinylpyrrolidone, 0.12 % Ficoll, 5 mM Na_2EDTA, 50 mM Tris/HCl, pH 7.4) containing 12 nM of the EBER PNA Probe/FITC (Y5200, DakoCytomation). Hybridization was carried out for 1 h at 56 °C. Then, the cells were washed twice and an Alexa Fluor 488 Signal Amplification kit (Molecular Probes) was used to enhance fluorescence and photostability. The stained cells were analysed using a FACSCalibur and CellQuest software (BD Biosciences). Up to 50 000 events were recorded for each analysis. The lymphocytes were gated by standard forward- and side-scatter profiles. Dead cells were not excluded. To determine the lower detection limit of the FISH assay for EBV$^+$ cells, we mixed EBV$^+$ Raji and EBV$^-$ BJAB cells in various ratios and quantified them by using the FISH assay (Kimura *et al.*, 2009). EBER-positive cells could be quantified, as the Raji/BJAB ratio was between 0.1 (EBV-positive cells were 10 %) and 0.0001 (0.01 %), although the population of CD19$^+$EBER$^+$ cells was less clear at a ratio of 0.0001. Therefore, the detection limit of the FISH assay was considered to be 0.01–0.1 %.

Statistical analyses were performed with SPSS for Windows version 18.0 (SPSS). Regression analysis (Pearson product-moment correlation coefficient) was used to compare the FISH assay and the real-time PCR. Values of $P<0.05$ were considered statistically significant.

The characteristics of each patient are shown in Table 1. Based on the FISH assay, EBER-positive lymphocytes were detected in all eight patients and they ranged from 0.05 to 0.78 % of lymphocytes (Table 1). The mean and SEM of the percentage of the EBER-positive cells was 0.27 ± 0.13 % in haematopoietic stem cell transplantation recipients and 0.38 ± 0.15 % in liver transplantation recipients. The phenotypes of each patient are also shown in Table 1. The percentage of the total of CD20$^+$ lymphocytes varies among patients, particularly in patients with haematopoietic stem cell transplant. In contrast, the percentages in the five healthy volunteers were within the normal range (14, 15, 19, 22 and 25). The EBV-infected cells were CD20$^+$IgD$^+$ or CD20$^+$CD27$^+$ cells in most patients. Representative results of the dual staining are shown in Fig. 1. In patient 2, EBER-positive lymphocytes were detected in 6 % of CD20$^+$ lymphocytes, and EBV-infected cells were mostly IgD$^+$ or CD27$^+$ cells. In patient 4, EBER-positive lymphocytes were detected in 2 % of CD20$^+$ lymphocytes, and EBV-infected cells were detected in approximately 50 % of IgD$^+$ or CD27$^+$ cells. The main EBV-infected cells were identified as being CD20$^+$IgD$^+$ or CD20$^+$CD27$^+$ cells in other patients. In contrast, EBER-positive cells were not detected in any of the five healthy volunteers (representative results are also shown in Fig. 1c, d), and the mean percentage of IgD$^+$ cells or CD27$^+$ cells within the sample of CD20$^+$ lymphocytes was 66 % (range, 56–78 %) and 48 % (range, 33–59 %), respectively.

Next, we compared the results of the FISH assay with those from the real-time quantitative PCR. The number of EBER-positive cells assayed by FISH was significantly correlated with the EBV-DNA load determined by real-time PCR ($r^2=0.88$, $P<0.0001$; Fig. 2).

The percentage of the total of CD20$^+$ cells in the five healthy volunteers was within the normal range, suggesting that the FISH assay was well performed. In contrast, these percentages vary among patients, particularly in patients with haematopoietic stem cell transplants (from 10 to 66 %, Table 1). Myeloablative chemotherapy followed by haematopoietic stem cell transplantation is associated with substantial B- and T-cell immunodeficiency for a period of up to several years (Douek *et al.*, 2000; Storek *et al.*, 1993). As the reconstitution of B- and T-cells was not parallel, and this reconstitution is influenced by various factors, such as graft-versus-host disease (Storek *et al.*, 2001), the ratio of these cells may vary in patients for prolonged periods after transplantation.

B-cells play a large role in the humoral immune response. Naïve B-cells proliferate and differentiate to yield memory

Table 1. Characteristics of haematopoietic stem cell/liver transplantation recipients with elevated EBV loads

EBER, EBV-encoded small RNA.

No.	Sex	Age (years)	Transplant	Clinical symptoms	Time post-transplant (months)	Time post testing EBV positive (months)	EBV DNA in PBMCs [copies (μg DNA)$^{-1}$]	$CD20^+$ lymphocytes (% of total)	$EBER^+$ lymphocytes (% of total)	Percentage of $CD20^+EBER^+$ lymphocytes		Percentage of $CD20^+EBER^-$ lymphocytes	
										IgD^+	$CD27^+$	IgD^+	$CD27^+$
1	F	7	Bone marrow	Fever, cough, diarrhoea	1	1	41,175	40	0.63	56	80	2	25
2	F	1	Bone marrow	Fever, diarrhoea, rash	3	1	3,730	15	0.10	83	100	16	40
3	F	6	Bone marrow	Malaise, cough, hilar lymphadenopathy	10	1	2,441	10	0.05	58	100	66	32
4	F	48	Cord blood	Hepatomegaly	37	6	10,500	66	0.28	48	49	8	6
5	M	1	Liver	Asymptomatic	9	8	13,392	29	0.39	81	99	11	23
6	F	2	Liver	Asymptomatic	15	15	4,729	12	0.15	79	99	67	40
7	F	2	Liver	Asymptomatic	15	15	8,302	23	0.19	83	98	64	36
8	M	10	Liver	Asymptomatic	96	96	16,438	36	0.78	68	83	27	20

B-cells and long-lived plasma cells in the course of a T-cell-dependent B-cell response. In humans, memory B-cells have mostly been characterized based on two surrogate markers of antigenic experience, namely the expression of isotype switched or somatically mutated immunoglobulins (Yoshida *et al.*, 2010). Human memory B-cells are predominantly identified by the expression of CD27 (Klein *et al.*, 1998). Mutated immunoglobulin sequences are found almost exclusively in $CD27^+$ B-cells, and CD27 is expressed on B-cells upon their activation (Klein *et al.*, 1998); however, it is absent from most cord-blood B-cells (Agematsu *et al.*, 1997). This may be the reason why the percentage of $CD20^+EBER^+CD27^+$ cells in patient 2 was much lower than that observed for other patients in the present study. Following this criteria, peripheral B-cells from adult blood or secondary lymphoid organs can be separated into 50–60 % naïve $CD27^-$ B-cells and 40–50 % $CD27^+$ memory cells. $CD27^+$ B-cells comprise $IgM^-IgD^-CD27^+$ class-switched cells (40 %) and two subsets (Yoshida *et al.*, 2010) of IgM memory cells: $IgM^+IgD^+CD27^+$ (40 %) and $IgM^+IgD^-CD27^+$ (20 %). In addition, a small fraction of IgD-only $CD27^+$ cells exists (<1 % of B-cells) (Yoshida *et al.*, 2010). Hochberg *et al.* (2004) reported that EBV mostly infected IgD^-CD27^+ B-cells (which appear to be $IgM^-IgD^-CD27^+$ class-switched cells or $IgM^+IgD^-CD27^+$ IgM memory cells) in patients with AIM, and this is the same as in latently EBV-infected cells from healthy carriers (Babcock *et al.*, 1998). In most cases of AIM, EBV-infected cells represented 10–50 % of circulating memory B-cells (Hochberg *et al.*, 2004). In this study, the EBV-infected cells were mostly $CD20^+IgD^+$, which appeared to be $IgM^+IgD^+CD27^+$ IgM memory cells. The phenotype of EBV-infected memory cells may differ in immunocompromised patients after transplantation compared with AIM patients. Alternatively, the composition of memory B-cell subsets in peripheral blood may be different between AIM patients and patients after stem cell/liver transplantation. Interestingly, the percentage of $EBER^+CD20^+CD27^+$ B-cells in patient 4, who underwent cord blood transplantation, was much less than in other patients. Further studies are needed to determine whether this difference leads to different clinical features.

In experiments with human B-lymphocytes, each EBV-infected cell was shown to contain one EBV episome 16 h after EBV infection (Alfieri *et al.*, 1991). With regard to cell lines, human lymphoblastoid X50-7 cells contain approximately five EBV genomes per cell (Arribas *et al.*, 1995). Raji cells, which were established in culture from a Burkitt's lymphoma biopsy, contain 50–60 genome equivalents per cell in latent form (Adams & Lindahl, 1975). By using a FISH assay with a specific probe for the *Bam*HI W region of EBV, Rose *et al.* (2002) measured the number of EBV genomes per infected cell in solid organ transplantation recipients with a persistent EBV load of 8–200 genomes per 10^5 PBMCs (low-load carriers) and with a persistent EBV load of more than 200 genomes per 10^5 PBMCs (high-load carriers). Low-load carriers had virus-infected cells harbouring one or two

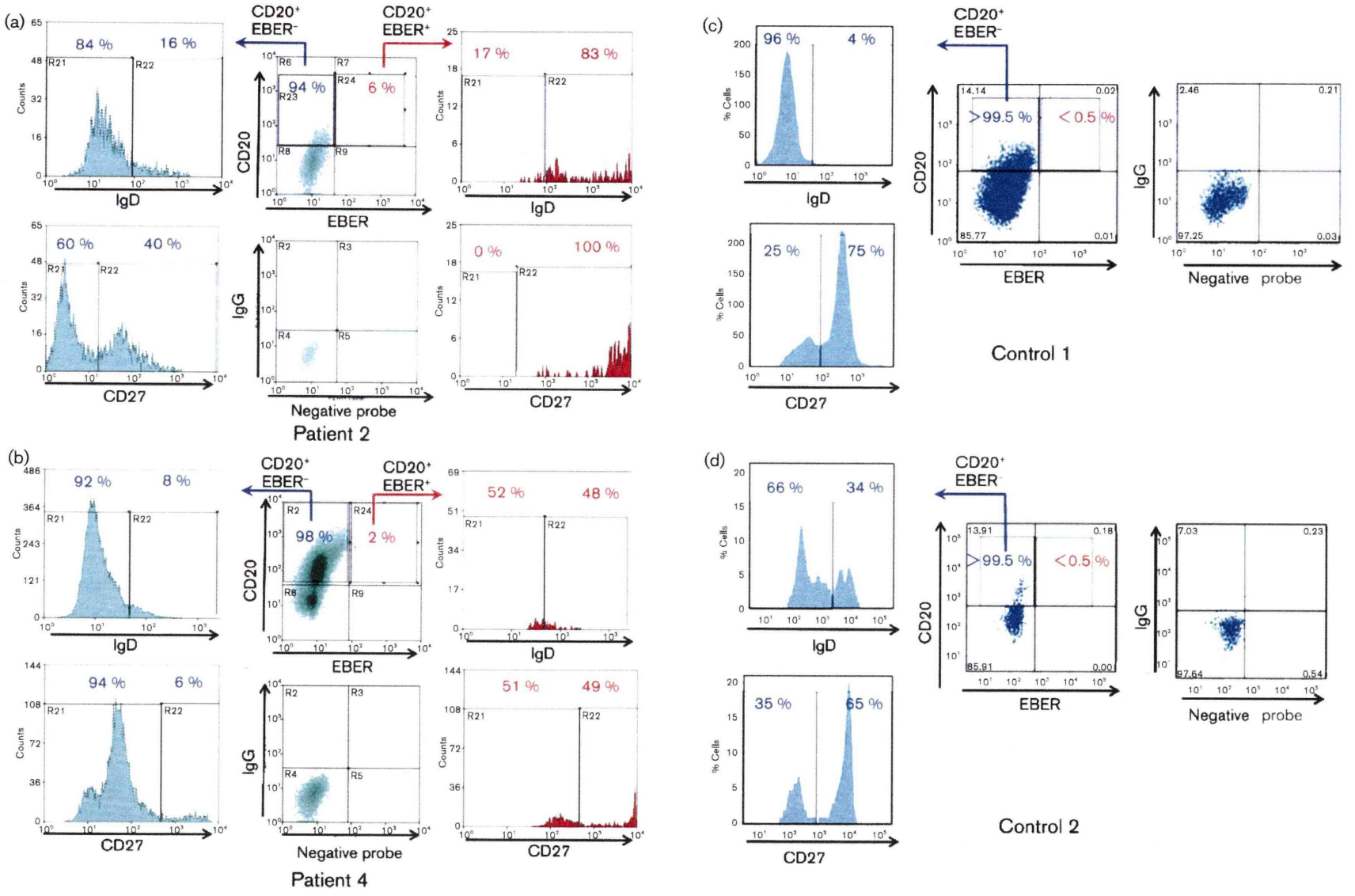

Fig. 1. Characterization of EBV-infected lymphocytes in representative patients. PBMCs were stained with mAbs for surface markers, fixed, permeabilized and hybridized with an EBER probe. The lymphocytes were gated by standard forward- and side-scatter profiles, and plotted on the quadrant that is at the centre of each panel for each patient or control. CD20$^+$EBER$^+$ lymphocytes (red) and CD20$^+$EBER$^-$ lymphocytes (blue) were gated and the expression of IgD or CD27 is shown in each histogram. (a) Patient 2; (b) patient 4; (c) control 1 (a healthy volunteer with a history of EBV infection); (d) control 2.

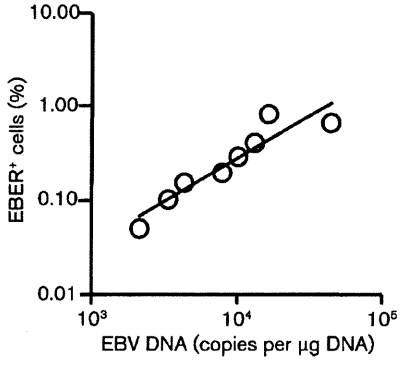

Fig. 2. Correlation between the percentage of EBER-positive lymphocytes, as measured by FISH, and the EBV-DNA load, as measured by using real-time PCR. EBER-positive lymphocytes in PBMCs from all eight patients were analysed by using the FISH assay. Amounts of EBV DNA in PBMCs from all eight patients were measured by using a real-time PCR assay.

genome copies per cell. High-load carriers had two populations of cells; one had one or two genome copies per cell and the other had more than ten copies per cell. By using another FISH assay, Calattini *et al.* (2010) reported that the average number of EBV genomes per cell in B-cells from patients with high EBV-DNA loads ranged from 7.3 to 22.25. EBV was also found at an approximately tenfold lower number of copies in T-cells than in B-cells. In the present study, the number of EBER-positive cells, measured by FISH, was significantly correlated with the EBV-DNA load determined by real-time PCR. As the number of EBERs is not correlated with the number of EBV genomes in infected cells, detection of EBERs does not provide a precise estimate of the number of EBV genomes present per cell. However, the number of EBV-genome equivalents can be calculated if the number of EBV genomes is equal in EBER-positive cells. Looking at the data in Fig. 2, 10^4 copies μg^{-1} of DNA points to the result that the percentage of EBER-positive cells is approximately 0.3 %. Because 1 μg DNA appears to be extracted from 2×10^5 PBMCs (Kimura *et al.*, 1999), 10^4 copies μg^{-1} of DNA is equivalent to 10^4 copies per 2×10^5 PBMCs, that is, five copies per 100 cells. If infected cells represent 0.3 % of cells, 16.7 copies of the EBV genome are in a single infected cell. Additionally, in a separate study we demonstrated a correlation between the number of EBER-positive cells, as measured by FISH, and the amount of EBV DNA in EBV-associated T- or NK-cell lymphoproliferative diseases, in which EBV infects T- or NK cells (unpublished data). The number of EBV genomes was estimated to be one tenth of that observed in the memory B-cells in this study (data not shown). These data are consistent with the results of Calattini *et al.* (2010). Characterizing the phenotype of EBV-infected cells by the FISH assay combined with a real-time PCR assay enables a quantitative analysis of EBV-associated diseases.

Acknowledgements

We thank Shuko Kumagai and Fumiyo Ando for excellent technical support. Potential conflicts of interest: The authors have no commercial or other associations that might pose a conflict of interest. Financial support: Japan Society for the Promotion of Science [Grant-in-Aid for Scientific Research (C) (20591276) to Y. Ito], and Ministry of Health, Labor, and Welfare of Japan [Grant for research on measures for emerging and re-emerging infections (Intractable Infectious Diseases in Organ Transplant Recipients, H21-Shinko-Ippan-009) to H. Kimura.]

References

Adams, A. & Lindahl, T. (1975). Epstein-Barr virus genomes with properties of circular DNA molecules in carrier cells. *Proc Natl Acad Sci U S A* 72, 1477–1481.

Agematsu, K., Nagumo, H., Yang, F. C., Nakazawa, T., Fukushima, K., Ito, S., Sugita, K., Mori, T., Kobata, T. & other authors (1997). B cell subpopulations separated by CD27 and crucial collaboration of $CD27^+$ B cells and helper T cells in immunoglobulin production. *Eur J Immunol* 27, 2073–2079.

Alfieri, C., Birkenbach, M. & Kieff, E. (1991). Early events in Epstein-Barr virus infection of human B lymphocytes. *Virology* 181, 595–608.

Arribas, J. R., Clifford, D. B., Fichtenbaum, C. J., Roberts, R. L., Powderly, W. G. & Storch, G. A. (1995). Detection of Epstein-Barr virus DNA in cerebrospinal fluid for diagnosis of AIDS-related central nervous system lymphoma. *J Clin Microbiol* 33, 1580–1583.

Babcock, G. J., Decker, L. L., Volk, M. & Thorley-Lawson, D. A. (1998). EBV persistence in memory B cells *in vivo*. *Immunity* 9, 395–404.

Bingler, M. A., Feingold, B., Miller, S. A., Quivers, E., Michaels, M. G., Green, M., Wadowsky, R. M., Rowe, D. T. & Webber, S. A. (2008). Chronic high Epstein-Barr viral load state and risk for late-onset posttransplant lymphoproliferative disease/lymphoma in children. *Am J Transplant* 8, 442–445.

Calattini, S., Sereti, I., Scheinberg, P., Kimura, H., Childs, R. W. & Cohen, J. I. (2010). Detection of EBV genomes in plasmablasts/plasma cells and non-B cells in the blood of most patients with EBV lymphoproliferative disorders by using immuno-FISH. *Blood* 116, 4546–4559.

D'Antiga, L., Del Rizzo, M., Mengoli, C., Cillo, U., Guariso, G. & Zancan, L. (2007). Sustained Epstein–Barr virus detection in paediatric liver transplantation. Insights into the occurrence of late PTLD. *Liver Transpl* 13, 343–348.

Douek, D. C., Vescio, R. A., Betts, M. R., Brenchley, J. M., Hill, B. J., Zhang, L., Berenson, J. R., Collins, R. H. & Koup, R. A. (2000). Assessment of thymic output in adults after haematopoietic stem-cell transplantation and prediction of T-cell reconstitution. *Lancet* 355, 1875–1881.

Gotoh, K., Ito, Y., Ohta, R., Iwata, S., Nishiyama, Y., Nakamura, T., Kaneko, K., Kiuchi, T., Ando, H. & Kimura, H. (2010). Immunologic and virologic analyses in pediatric liver transplant recipients with chronic high Epstein–Barr virus loads. *J Infect Dis* 202, 461–469.

Green, M., Soltys, K., Rowe, D. T., Webber, S. A. & Mazareigos, G. (2009). Chronic high Epstein–Barr viral load carriage in pediatric liver transplant recipients. *Pediatr Transplant* 13, 319–323.

Hochberg, D., Souza, T., Catalina, M., Sullivan, J. L., Luzuriaga, K. & Thorley-Lawson, D. A. (2004). Acute infection with Epstein-Barr virus targets and overwhelms the peripheral memory B-cell compartment with resting, latently infected cells. *J Virol* 78, 5194–5204.

Kimura, H., Morita, M., Yabuta, Y., Kuzushima, K., Kato, K., Kojima, S., Matsuyama, T. & Morishima, T. (1999). Quantitative analysis of

Epstein–Barr virus load by using a real-time PCR assay. *J Clin Microbiol* **37**, 132–136.

Kimura, H., Miyake, K., Yamauchi, Y., Nishiyama, K., Iwata, S., Iwatsuki, K., Gotoh, K., Kojima, S., Ito, Y. & Nishiyama, Y. (2009). Identification of Epstein–Barr virus (EBV)-infected lymphocyte subtypes by flow cytometric in situ hybridization in EBV-associated lymphoproliferative diseases. *J Infect Dis* **200**, 1078–1087.

Klein, U., Rajewsky, K. & Küppers, R. (1998). Human immunoglobulin (Ig)M$^+$IgD$^+$ peripheral blood B cells expressing the CD27 cell surface antigen carry somatically mutated variable region genes: CD27 as a general marker for somatically mutated (memory) B cells. *J Exp Med* **188**, 1679–1689.

Kurth, J., Spieker, T., Wustrow, J., Strickler, G. J., Hansmann, L. M., Rajewsky, K. & Küppers, R. (2000). EBV-infected B cells in infectious mononucleosis: viral strategies for spreading in the B cell compartment and establishing latency. *Immunity* **13**, 485–495.

Rickinson, A. B. & Kieff, E. (2006). Epstein-Barr virus. In *Fields Virology*, 5th edn, pp. 2655–2700. Edited by D. M. Knipe & P. M. Howley. Philadelphia, PA: Lippincott Williams & Wilkins.

Rose, C., Green, M., Webber, S., Kingsley, L., Day, R., Watkins, S., Reyes, J. & Rowe, D. (2002). Detection of Epstein–Barr virus genomes in peripheral blood B cells from solid-organ transplant recipients by fluorescence in situ hybridization. *J Clin Microbiol* **40**, 2533–2544.

Storek, J., Ferrara, S., Ku, N., Giorgi, J. V., Champlin, R. E. & Saxon, A. (1993). B cell reconstitution after human bone marrow transplantation: recapitulation of ontogeny? *Bone Marrow Transplant* **12**, 387–398.

Storek, J., Wells, D., Dawson, M. A., Storer, B. & Maloney, D. G. (2001). Factors influencing B lymphopoiesis after allogeneic hematopoietic cell transplantation. *Blood* **98**, 489–491.

Thorley-Lawson, D. A. & Gross, A. (2004). Persistence of the Epstein–Barr virus and the origins of associated lymphomas. *N Engl J Med* **350**, 1328–1337.

Wada, K., Kubota, N., Ito, Y., Yagasaki, H., Kato, K., Yoshikawa, T., Ono, Y., Ando, H., Fujimoto, Y. & other authors (2007). Simultaneous quantification of Epstein–Barr virus, cytomegalovirus, and human herpesvirus 6 DNA in samples from transplant recipients by multiplex real-time PCR assay. *J Clin Microbiol* **45**, 1426–1432.

Yoshida, T., Mei, H., Dörner, T., Hiepe, F., Radbruch, A., Fillatreau, S. & Hoyer, B. F. (2010). Memory B and memory plasma cells. *Immunol Rev* **237**, 117–139.

OPEN ACCESS Freely available online

PLoS one

Replication of Epstein-Barr Virus Primary Infection in Human Tonsil Tissue Explants

Kensei Gotoh[1], Yoshinori Ito[1]*, Seiji Maruo[2], Kenzo Takada[2], Terukazu Mizuno[3], Masaaki Teranishi[3], Seiichi Nakata[3], Tsutomu Nakashima[3], Seiko Iwata[4], Fumi Goshima[4], Shigeo Nakamura[5], Hiroshi Kimura[4]

1 Department of Pediatrics, Nagoya University Graduate School of Medicine, Nagoya, Japan, **2** Department of Tumor Virology, Institute for Genetic Medicine, Hokkaido University, Sapporo, Japan, **3** Department of Otorhinolaryngology, Nagoya University Graduate School of Medicine, Nagoya, Japan, **4** Department of Virology, Nagoya University Graduate School of Medicine, Nagoya, Japan, **5** Department of Pathology and Laboratory Medicine, Nagoya University Hospital, Nagoya, Japan

Abstract

Epstein-Barr virus (EBV) may cause a variety of virus-associated diseases, but no antiviral agents have yet been developed against this virus. Animal models are thus indispensable for the pathological analysis of EBV-related infections and the elucidation of therapeutic methods. To establish a model system for the study of EBV infection, we tested the ability of B95–8 virus and recombinant EBV expressing enhanced green fluorescent protein (EGFP) to replicate in human lymphoid tissue. Human tonsil tissues that had been surgically removed during routine tonsillectomy were sectioned into small blocks and placed on top of collagen sponge gels in culture medium at the air-interface, then a cell-free viral suspension was directly applied to the top of each tissue block. Increasing levels of EBV DNA in culture medium were observed after 12–15 days through 24 days post-infection in tissue models infected with B95–8 and EGFP-EBV. Expression levels of eight EBV-associated genes in cells collected from culture medium were increased during culture. EBV-encoded small RNA-positive cells were detected in the interfollicular areas in paraffin-embedded sections. Flow cytometric analyses revealed that most $EGFP^+$ cells were $CD3^-$ $CD56^-$ $CD19^+$ $HLA\text{-}DR^+$, and represented both naïve (immunoglobulin D^+) and memory ($CD27^+$) B cells. Moreover, EBV replication in this model was suppressed by acyclovir treatment in a dose-dependent manner. These data suggest that this model has potential for use in the pathological analysis of local tissues at the time of primary infection, as well as for screening novel antiviral agents.

Citation: Gotoh K, Ito Y, Maruo S, Takada K, Mizuno T, et al. (2011) Replication of Epstein-Barr Virus Primary Infection in Human Tonsil Tissue Explants. PLoS ONE 6(10): e25490. doi:10.1371/journal.pone.0025490

Editor: Luwen Zhang, University of Nebraska – Lincoln, United States of America

Received February 25, 2011; **Accepted** September 6, 2011; **Published** October 5, 2011

Funding: This study was supported by grants from the Japan Society for the Promotion of Science (20591276) to YI and from Health and Labour Science Research (22091401) to YI and HK. The funders had no role in study design, data collection and analysis, decision to publish, or preparation of the manuscript.

Competing Interests: The authors have declared that no competing interests exist.

* E-mail: yoshi-i@med.nagoya-u.ac.jp

Introduction

Epstein-Barr Virus (EBV) is a universal human γ-herpesvirus, generally transmitted via saliva, with the oropharynx as the site of infection [1,2]. Primary EBV infection occurs most frequently in infancy and childhood, and in many cases causes either no or only nonspecific symptoms. In cases of primary infection among adolescents and young adults, infectious mononucleosis (IM) often develops, and the course may sometimes be severe or fatal. After infection, EBV remains in most adults as an asymptomatic latent infection, but may cause neoplastic disorders such as Burkitt's lymphoma or post-transplant lymphoproliferative disorder (PTLD).

Although EBV may cause a variety of disorders, no vaccine or antiviral agent has yet been developed against this virus [1,2]. In general, animal models are indispensable for the pathological analysis of viral infections and the elucidation of methods of treatment and prevention, but EBV only infects humans in nature and limited animal species under experimental conditions. Various infection models have been used to investigate EBV-associated diseases [3,4,5,6,7]. Mouse models that partially reconstitute human immune system components after engagement of hematopoietic progenitor cells are of particular interest, because they reproduce human immunity and diseases caused by EBV. Several mouse models of immunodeficiency have been applied, including $Rag2^{-/-}$ $\gamma c^{-/-}$ mice [8,9], NOD/SCID mice [10], NOD/SCID/$\gamma c^{-/-}$ mice [11,12,13], BLT mice (NOD/SCID mice with implantation of human fetal liver and thymus pieces under the renal capsule) [14], and NOD/Shi-SCID/IL-2Rγ^{null} (NOG) mice [15]. Of these, the NOG mice model [15] has been used to show that B-cell lymphoproliferative disorder arises during EBV infection with a high viral load, whereas asymptomatic persistent infection arises from infection with a low viral load. In addition, EBV-specific T-cell responses and EBV-specific antibodies were detected in blood, revealing this mouse model as a useful tool for investigating the pathogenesis, prevention, and treatment of EBV infection. Culture models using human lymphatic tissues, however, appear advantageous for the study of localized pathology in EBV infection. We therefore focused on a model of infection using human tonsillar lymphoid tissues.

Numerous reports have described the use of viral infection models using human tonsillar lymphoid tissues for the study of human immunodeficiency virus (HIV) [16], while others have described the use of such models for investigating other members

of the herpesvirus family, such as human herpesvirus (HHV)-6, HHV-7, and herpes simplex virus (HSV)-2 [17,18,19]. The palatine tonsils comprise typical lymphoid tissue and are also the natural portal of entry for EBV, thus showing great potential for reproducing the pathology of primary infection with EBV. The present study used human tonsillar lymphoid tissues to establish an EBV infection model and investigated infected cells during the initial stage of infection. We also tested the utility of this model as a screening system for antiviral agents.

Materials and Methods

Ethics statement

Human subject protocols were approved by the institutional review board of Nagoya University School of Medicine (2006-450). Written informed consent was provided by study participants and/or their legal guardians prior to enrolment.

Virus stocks

Cell-free virus solution was obtained from culture supernatant of B95–8 cells (an EBV-infected marmoset cell line) (ATCC) after centrifuging for 5 min at 3,000×*g* and filtration through a 0.45-μm membrane filter. In some experiments, we also used supernatants containing recombinant EBV expressing enhanced green fluorescent protein (EGFP), in which a gene cassette consisting of the EGFP gene driven by the simian virus 40 promoter and a neomycin resistance gene driven by the simian virus 40 promoter were inserted into the viral BXLF1 gene [20]. Titers of virus in the 50% transforming dose (TD_{50}) were determined using the Reed-Muench method, as described elsewhere [15,21]. Calculated titers were 1×10^2 TD_{50}/ml for B95 and 1×10^3 TD_{50}/ml for EGFP-EBV.

Tissue culture and viral infection

Human tonsils surgically removed during routine tonsillectomy and not required for clinical purposes were received within several hours of excision, then dissected, cultured, and infected, as described elsewhere [16,22,23]. Since EBV-specific immune responses may impact cellular infection, we only used tonsils from EBV-seronegative individuals. Serological tests for anti-EBV antibodies were examined 2–4 weeks preoperatively and negative results for viral capsid antigen immunoglobulin (Ig) G and EBV nuclear antigen were confirmed. In brief, the tonsils were washed thoroughly with medium containing antibiotics, sectioned into cubes with an average weight of 5 mg, and placed on top of collagen sponge gels in culture medium at the air-interface. For EBV infection, 10 μL of clarified viral suspension was directly applied on top of each tissue block. The culture medium used to bathe 54 tissue blocks in six wells was collected every 3 days after viral inoculation. Cell-free supernatants and cells were obtained after centrifugation of collected medium and used for the following assays. Cells collected from culture medium were considered to have come from infected tissues. Most of the epithelial tonsillar layers were lost during preparation of tissue blocks, so replication of EBV in epithelial cells could not be examined.

Quantification of EBV DNA

Viral DNA was extracted from either 200 μL of cell-free culture supernatants or from 5×10^5 cells collected from culture medium using QIAamp DNA blood kits (Qiagen). Real-time quantitative PCR assays were performed as previously described [24,25,26].

RNA purification and real-time RT-PCR

RNA was extracted from 5×10^5 cells from culture medium with a QIAmp RNeasy Mini Kit (Qiagen). Viral mRNA expression was quantified by one-step multiplex real-time reverse transcription (RT)-PCR using the Mx3000P real-time PCR system (Stratagene), as described previously [27,28], to examine expression levels of two lytic genes (BZLF1 and gp350/220) and six latent genes (EBV-encoded nuclear antigen (EBNA)1, EBNA2, latent membrane protein (LMP)1, LMP2, EBV-encoded small RNA (EBER)1, and *Bam*HI-A rightward transcripts (BARTs)). The stably expressed housekeeping gene β_2-microglobulin (*β2M*) was used as an endogenous control and reference gene for relative quantification. Each experiment was conducted in triplicate and results are shown as the mean of three samples with standard errors.

Immunohistology and *in situ* hybridization

Tissue blocks were fixed with 10% buffered formalin, embedded in paraffin, and sectioned at 5 μm and stained with hematoxylin and eosin (HE). The monoclonal antibodies used were anti-CD3, anti-CD20, anti-follicular dendritic cell (FDC), EBNA2, LMP1 and BZFL1 (Dako), all of which were used after antigen retrieval following heating in a microwave oven [27,29]. *In situ* hybridization was performed using the EBER1 probe (Dako) as previously described [24,27]. Hybridization was detected using mouse monoclonal anti-fluorescein isothiocyanate (Dako) and a Vectastain ABC kit (Vector). For both immunostaining and *in situ* hybridization, diaminobenzidine was used for visualization.

Flow cytometry

At day 15–24 post-infection with EGFP-EBV, single-cell suspensions were dissected from tissue blocks by mechanical dissociation. Tissue blocks were placed into a petri plate with complete medium and gently ground with pestles. As shown previously, this procedure releases lymphocytes from stromal elements [23]. Similarly, cells that had emigrated into the collagen sponge were mechanically squeezed out and collected by centrifugation. Cell debris and fragments were removed and mononuclear cells (MNCs) were purified by Ficoll-Hypaque centrifugation [30]. MNCs were washed three times and stained using a combination of the following monoclonal antibodies (mAbs): phycoerythrin (PE)-labeled anti-CD19 (clone HD37; Dako); anti-CD3 (clone UCHT1; eBioscience); anti-CD56 (clone IM2073; Beckman Coulter); PE-cyanin 5 (PC5)-labeled anti-CD56 (clone IM2654; Beckman Coulter); and anti-HLA-DR (clone IMMU357; Beckman Coulter). In a few experiments, collected cells were also stained with 7-amino-actinomycinD (7-AAD; BD Pharmingen) at day 24, to exclude dead cells on samples. Discrimination between infection with memory or naive B cells was determined using the following antibody combination: PE-labeled anti-CD27 (clone M-T271; Becton Dickinson); anti-IgD (clone IgD26; Miltenyi Biotec); and PC5-labeled anti-CD19 (clone HIB19; eBioscience). Isotype-matched monoclonal mouse IgG antibodies were used in each experiment as controls. Stained cells were analyzed using FACSCalibur and CellQuest version 5.2.1 software (Becton Dickinson).

Acyclovir (ACV) treatment

To test the anti-EBV activity of ACV (GlaxoSmithKline), B95-infected tissue blocks were incubated with culture medium containing ACV at various concentrations (1.5, 5, 15 or 45 μg/ml). Culture medium was changed every 3 days after viral inoculation, and ACV was added with every medium change. A

sample of medium collected from each exchange was used for quantification of EBV DNA, as previously mentioned.

Flow cytometric in situ hybridization (FISH) assay

To quantify EBV-infected cells and to analyze the cell types of EBV-infected populations, FISH assays were used [31]. Briefly, 5×10^5 MNCs were stained with phycoerythrin cyanine 5 (PC5)-labeled anti-CD45 (clone HI30; Biolegend) monoclonal antibodies for 1 h at 4°C. Isotype-matched monoclonal mouse IgG antibodies were used as controls. After staining with antibodies, cells were fixed with 1% acetic acid/4% paraformaldehyde, permeabilized with 0.5% Tween 20/phosphate-buffered saline, and hybridized with a fluorescein-labeled EBER-specific peptide nucleic acid probe (Y5200; Dako). Fluorescence intensity was enhanced using the AlexaFluor 488 Signal Amplification Kit (Molecular Probes), and stained cells were analyzed using FACSCalibur and CellQuest software (BD Biosciences).

Statistical analyses

Data are presented as means ± standard error of the mean. Statistical analyses were conducted using StatView version 5.0

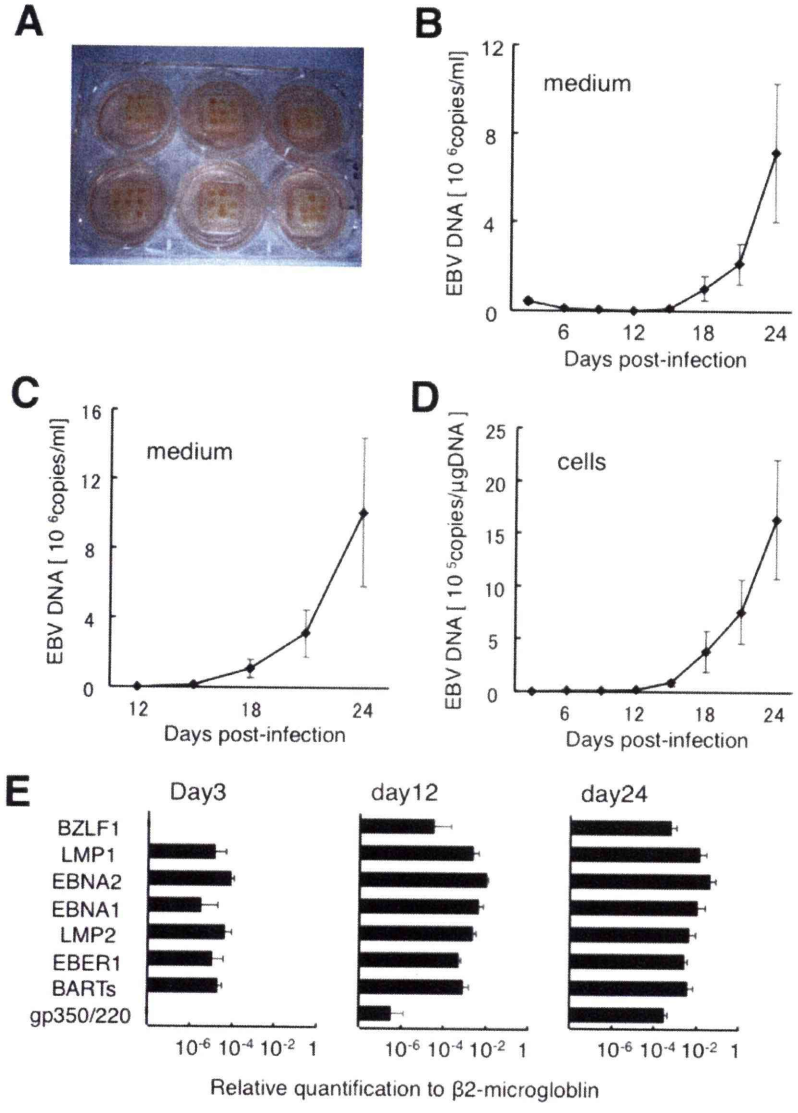

Figure 1. Kinetics of EBV DNA and expression patterns of EBV-related genes in human tonsil tissue explants infected with B95-8. Culture medium was changed every 3 days, and collected medium was centrifuged. Cell-free supernatants and cells collected from culture medium were used for quantification of EBV DNA by real-time PCR assay and quantification of viral mRNA by real-time RT-PCR assay. Data are presented as mean ± standard error of the mean. **A**) Tissue blocks on top of collagen sponge gels in a six-well plate. **B**) Kinetics of EBV DNA in cell-free supernatants. Average data were obtained from tissues derived from 12 donors. **C**) Plots of accumulated EBV DNA in cell-free culture medium after day 12 post-infection ($n=12$). **D**) Kinetics of EBV DNA in cells from medium ($n=12$). **E**) Levels of EBV-related gene expressions in cells at 3, 12, and 24 days post-infection ($n=4$).
doi:10.1371/journal.pone.0025490.g001